AD-A069 545 PRINCETON UNIV NJ DEPT OF MECHANICAL AND AEROSPACE --ETC F/G 21/8.2
RESEARCH ON UNSTEADY COMBUSTION PROCESSES.(U)
NOV 78 L H CAVENY, A GANY, M M MICCI AFOSR-76-3104
UNCLASSIFIED AFOSR-TR-79-0548 NL

| OF |
ADA
069 545

END
DATE
FILMED
7-79
DDC

LEVEL II

ANNUAL REPORT TO THE
AIR FORCE OFFICE OF SCIENTIFIC RESEARCH

on

RESEARCH ON UNSTEADY COMBUSTION PROCESSES

AFOSR Grant AF-76-3104
From 1 October 1977 to 30 September 1978

November 1978

Authors

L. H. Caveny, A. Gany and M. M. Micci

Submitted by

Leonard H. Caveny
Senior Professional Technical
Staff Member

Approved for Public Release: Distribution Unlimited

Department of Mechanical and Aerospace Engineering
PRINCETON UNIVERSITY
Princeton, New Jersey

UNCLASSIFIED

SECURITY CLASSIFICATION OF THIS PAGE (When Data Entered)

REPORT DOCUMENTATION PAGE	READ INSTRUCTIONS BEFORE COMPLETING FORM
1. REPORT NUMBER: AFOSR-TR-79-0548	2. GOVT ACCESSION NO. / 3. RECIPIENT'S CATALOG NUMBER
4. TITLE (and Subtitle): RESEARCH ON UNSTEADY COMBUSTION PROCESSES	5. TYPE OF REPORT & PERIOD COVERED: Annual rept. 1 Oct 77 - 30 Sep 78 / 6. PERFORMING ORG. REPORT NUMBER
7. AUTHOR(s): LEONARD H. CAVENY, ALON GANY, MICHAEL M. MICCI	8. CONTRACT OR GRANT NUMBER(s): AFOSR-76-3104
9. PERFORMING ORGANIZATION NAME AND ADDRESS: PRINCETON UNIVERSITY, MECHANICAL & AEROSPACE ENGINEERING DEPARTMENT, PRINCETON, NJ 08540	10. PROGRAM ELEMENT, PROJECT, TASK AREA & WORK UNIT NUMBERS: 2308/A1, 61102F / A1
11. CONTROLLING OFFICE NAME AND ADDRESS: AIR FORCE OFFICE OF SCIENTIFIC RESEARCH/NA, BLDG 410, BOLLING AIR FORCE BASE, D C 20332	12. REPORT DATE: Nov, 78 / 13. NUMBER OF PAGES: 50
14. MONITORING AGENCY NAME & ADDRESS (if different from Controlling Office)	15. SECURITY CLASS. (of this report): UNCLASSIFIED / 15a. DECLASSIFICATION/DOWNGRADING SCHEDULE

16. DISTRIBUTION STATEMENT (of this Report)

Approved for public release; distribution unlimited.

17. DISTRIBUTION STATEMENT (of the abstract entered in Block 20, if different from Report)

18. SUPPLEMENTARY NOTES

19. KEY WORDS (Continue on reverse side if necessary and identify by block number)

SOLID PROPELLANT ROCKET MOTORS
UNSTEADY COMBUSTION
COMBUSTION INSTABILITY
ALUMINUM COMBUSTION
ALUMINUM AGGLOMERATION

410 732

20. ABSTRACT (Continue on reverse side if necessary and identify by block number)

Nonsteady propellant combustion and chamber flow behavior, particularly as they relate to combustion stability and aluminized propellant combustion are being studied. The first part of the study is centered around the modulated throat rocket motor which is being developed to investigate the dynamic responses of high performance rocket motors in which externally excited longitudinal pressure and velocity waves produce couplings with propellant combustion processes. Transfer functions between the measured head-end and nozzle-end pressures produce gain and phase information in the vicinity of the first 3 harmonics. The

corresponding analytical models now being developed take into account the couplings of nonsteady chamber flow, nozzle flow, dynamic burning, and velocity coupling. In the second part of the study, combustion and agglomeration processes of aluminum particles emitted from the surface of aluminized propellants are being studies under rocket motor, crossflow conditions. High-speed, color photographs (≈4000 fr/s) are being taken of burning Al/Al_2O_3 agglomerates forming on the surface, moving along the surface, and entering the flowfield. The aluminum agglomeration and ignition processes are being interpreted in terms of a phenomenological model.

PREFACE

This is the annual report issued under Grant AF-76-3104 from the Energetics Division of the Air Force Office of Scientific Research. The period of performance was 1 October 1977 to 30 September 1978. The technical monitors for the program were Dr. J. F. Masi and Capt. R. F. Sperlein, USAF.

TABLE OF CONTENTS

1.0 INTRODUCTION AND TECHNICAL OBJECTIVES

Propellant combustion and chamber flow behavior, particularly as they relate to combustion stability and aluminum burning in solid rockets, are being studied. The experimental techniques and the analytical models are being developed to take into account the couplings such as unsteady chamber flow, nozzle flow, dynamic burning, and velocity coupling. Aluminum agglomerates as they form on the propellant surface and after they leave the propellant surface and enter the high velocity port flow are being studied using improved high-speed photographic techniques. Since the results are being obtained using rocket motor configurations and high energy propellants, the experiments are producing propellant/chamber response characteristics that should be readily relatable to developmental rocket motors.

The studies summarized in this annual report seek to further the scientific understanding of propellant combustion and chamber flow behavior, particularly as they relate to unsteady combustion and flow in high-performance rocket motors. As an example of the practical objectives, the results of such research can be important inputs to procedures to optimize propellant geometry, operating pressure, propellant formulations, etc. Also, the results can lead to generalizations of this knowledge for applications to new, advanced propellants and new rocket motor concepts. An equally powerful motivation for the research is the scientific one. The phenomena that occur in many unsteady flame and reacting flow field situations have not been adequately explained in terms of physical models and theories. In this sense, the problems of unsteady flow and combustion processes in solid rocket chambers represent a scientific challenge. Solutions to these problems will have important implications even for the supposedly well-understood cases of steady state flames. All of this suggests that the exploration of unsteady phenomena will lead to a much more advanced understanding of the physicochemical and fluid mechanical bases of flames and chamber flows.

2.0 CURRENT RESEARCH

2.1 Solid Propellant Rocket Motor Response Functions Evaluated by Means of Forced Longitudinal Waves

A methodology centered around the modulated throat rocket motor (MTRM) is being developed to investigate and categorize the dynamic responses of high performance rocket motors in which the avoidance of longitudinal mode combustion instability is a consideration. The modulated throat rocket motor establishes (under controlled conditions) periodic longitudinal pressure and velocity oscillations in rocket chambers having small port-to-throat area ratios. The oscillations are set up by alternately restricting and opening a conventional sonic-nozzle throat by means of a slotted, rotating wheel (see Fig. 1). The rocket motors used in the experiments have high loading densities and are not specially devised apparatuses for testing propellants isolated from the rocket motor chamber environment. As such,

(a) Heat losses are minimized.

(b) The important couplings between the propellant surface close-in flame zone, and chamber reactions occur naturally.

(c) Velocity and pressure coupling effects and their interactions are coupled to the mean chamber flow.

Since tests are conducted over the entire duty cycle of motor operation, a single test can survey a range of L*'s, internal Mach numbers, and propellant cavity geometries.

The objectives for developing and analyzing the modulated throat rocket motor in which longitudinal waves are important include:

(1) to determine from measurements the amplitude ratio and phase relationship of the head-end and nozzle-end pressure responses for a range of motor, excitation, and propellant conditions.

(2) to develop a non-linear mathematical model that uses experimentally correlated response functions (obtained by other laboratories) to predict the pressure and velocity distribution in the MTRM.

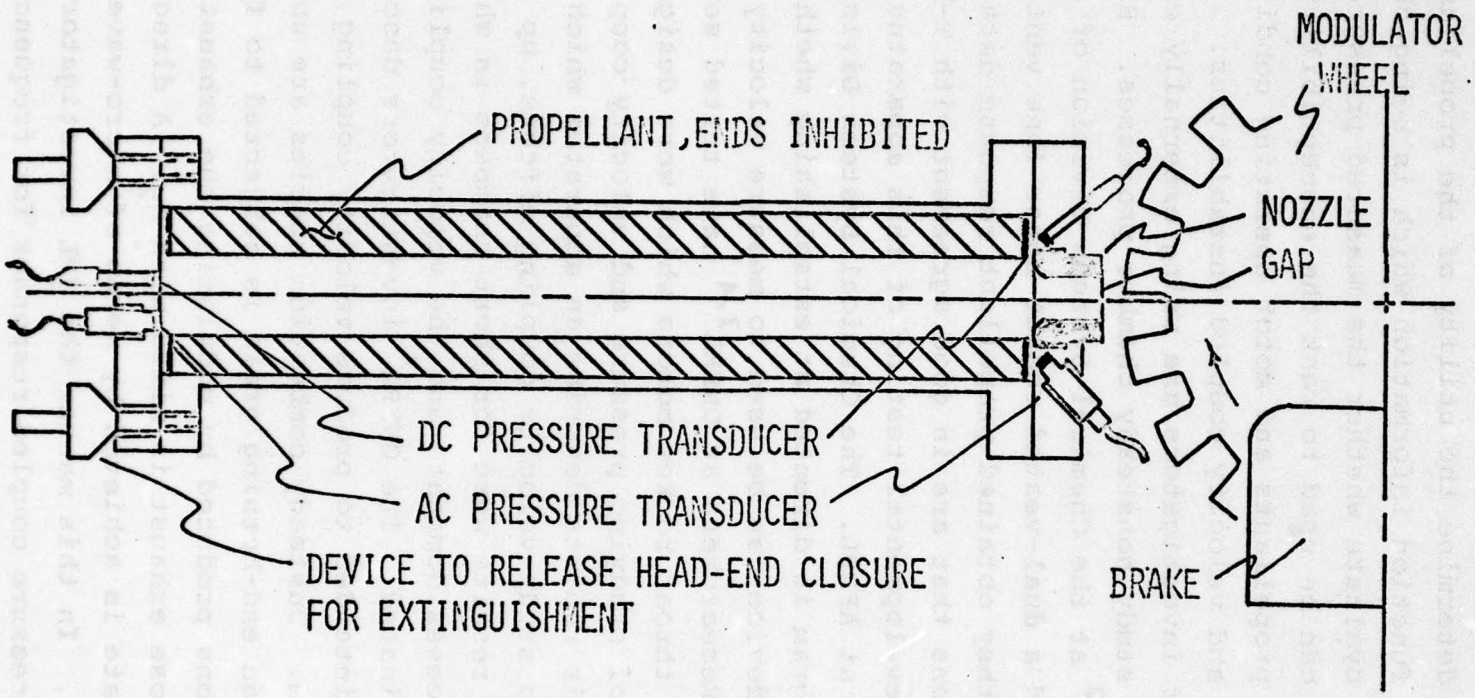

Fig. 1 Major components of Modulated Throat Rocket Motor.

(3) to compare the results of Objectives 1 and 2 to determine the utility of the propellant response function information which is being obtained and to evaluate whether the measured pressure response data can be used to rank the susceptibility of candidate propellants and motor operating conditions to pressure and velocity coupled instabilities.

Other investigators are using externally excited rocket motors to study nonsteady chamber processes. Brown and co-workers[1,2] at the Chemical Systems Division of United Technologies used a dual-vented rocket motor (one vent is modulated) in which they obtained propellant response data for bulk mode oscillations that are in good agreement with T-burner results. Further developmental testing of this apparatus is being conducted at AFRPL. The Chemical Systems Division present AFOSR program is directed at establishing whether a dual-throated device can be used to measure velocity coupling responses. Researchers at ONERA[3,4] have tested several types of modulated throat rocket motors which were designed for the purposes of studying pressure and velocity coupled responses. While their reports describe an apparatus which could possibly be used to study velocity coupling effects, up to 1976 their published results were for short chambers in which the bulk mode processes dominate and the velocity coupling effects have been eliminated. The ONERA[4] investigators described an apparatus which is intended to produce velocity coupling under controlled conditions. Unsteady combustion studies are underway at JPL[5] in which an end-burning grain is subjected to forced pressure oscillations produced by modulating the exhaust vent of a combustor whose exhaust is mixed with N_2. A direct measure of burning rate is achieved by means of micro-wave reflection technique. In this manner the JPL investigators are able to measure pressure coupled responses for frequencies less than about 200 Hz. The work being carried out at Princeton University goes beyond the pressure and velocity coupling studies reported by other laboratories. Our effort is directed at

velocity coupled responses and chamber/propellant interactions resulting from the combustion gases flowing in high performance motors in which longitudinal waves can be sustained.

2.1.1 Apparatus

As shown in Fig. 1, the major components of the MTRM are: (1) a conventional rocket motor with a sonic throat (in the present case, 25, 30, and 50 cm long motors are being used), (2) the modulating wheel assembly (includes electric motor drive, speed control, and nozzle gap adjustments), and (3) special head-end and nozzle-end closures for flush-mounted pressure transducer.

The modulating wheel assemblies are modules that can be used in conjunction with a variety of rocket motors. Indeed, our plans call for using the modulating wheel with a 50 cm slab motor to obtain pressure measurements at several axial positions. Special purpose instrumentation and computer programs were developed and implemented to acquire and analyze the low amplitude pressure versus time data with sufficient accuracy. The amplified output from high frequency, high output level (miniature) strain gauge-type pressure transducers are recorded using two methods: (1) on a Honeywell 5600C analog tape recorder at 60 ips and a band width of 10 kHz, and (2) digitized at rates of 140,000 12 bit words/sec and acquired by a Hewlett Packard 1000 Series computer. The pressure data are acquired in two forms, i.e., the absolute pressure and the unsteady component. Since steady state oscillations are set up, only selected portions of the record are required for data reduction using the HP digital computer. The data reduction procedure consists of Fourier analysis of head-end and nozzle-end pressures, (i.e., p_{head} and p_{noz}), cross-correlation of the Δp_{head} and Δp_{noz}, and development of forcing functions for use in the analytical model. Figure 2 is a schematic diagram of the data analysis steps. Figure 3 illustrates the type of wave forms that are developed in the head- and nozzle-ends of a progressively burning motor.

DATA REDUCTION STEPS
AFTER DATA HAS BEEN DIGITIZED AND STORED

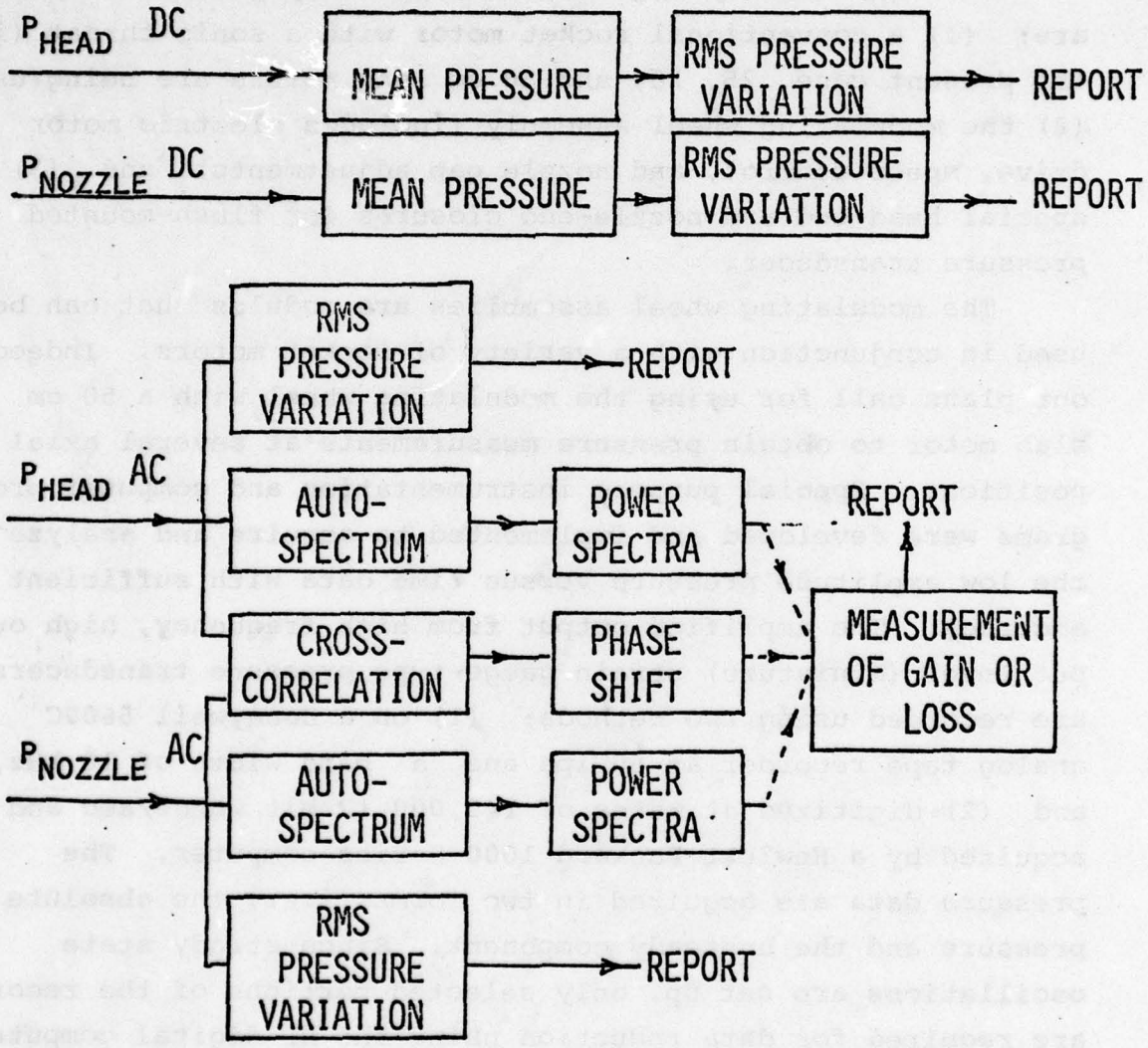

Fig. 2 Steps taken in analysis of data from modulated throat rocket motor.

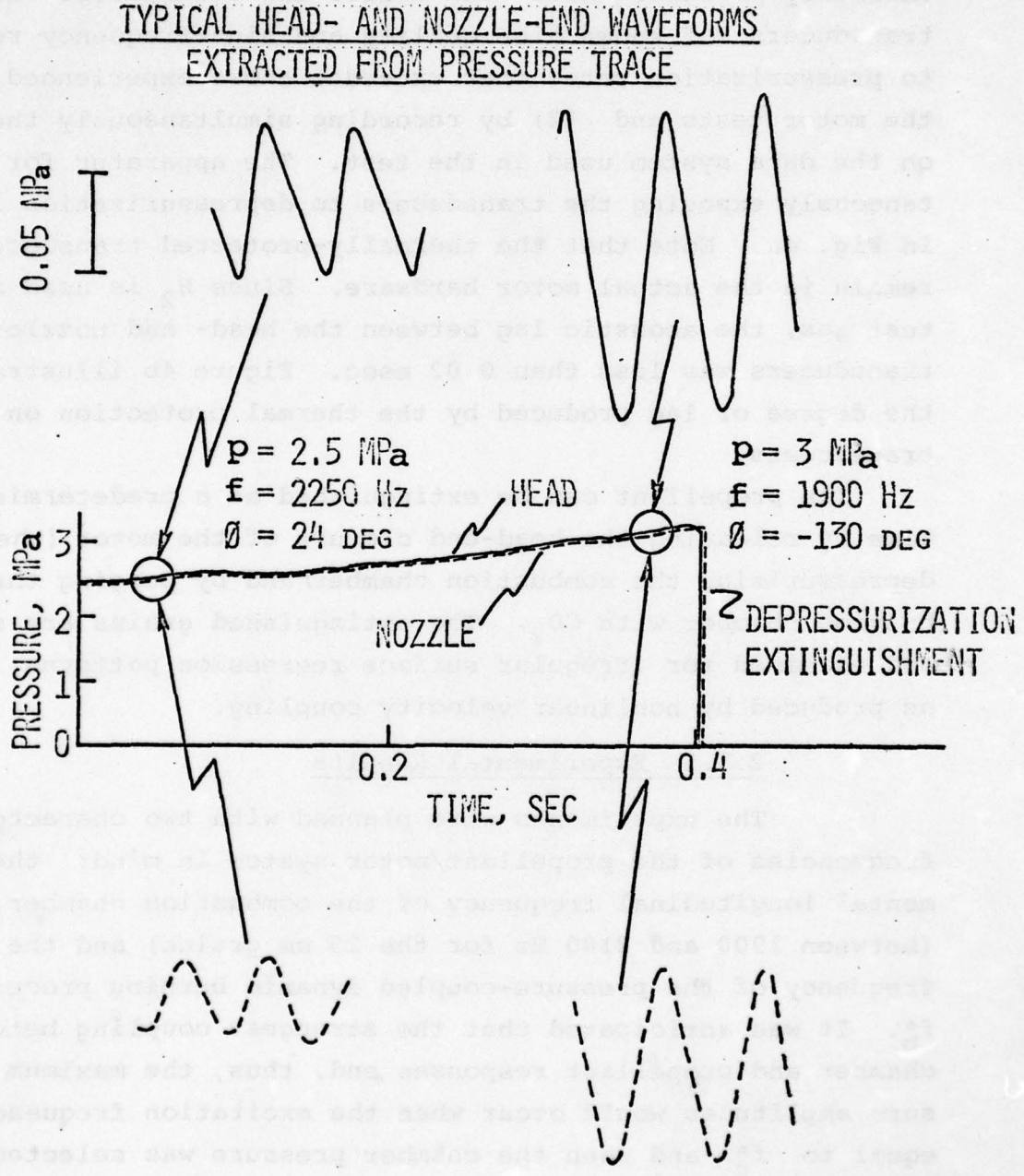

Fig. 3 Typical head- and nozzle-end wave forms measured during experiment.

In addition to the routine static calibrations, a necessary part of this study was an end-to-end dynamic calibration of the transducers and data-recording complex as it was used in the motor tests. This was accomplished by (1) exposing both the thermally protected head- and nozzle-end transducers and bare transducers (of known high quality and high-frequency response) to pressurization rates that exceeded those experienced during the motor tests and (2) by recording simultaneously the data on the data system used in the test. The apparatus for simultaneously exposing the transducers to depressurization is shown in Fig. 4a. Note that the thermally-protected transducers remain in the actual motor hardware. Since H_2 is used as the test gas, the acoustic lag between the head- and nozzle-end transducers was less than 0.02 msec. Figure 4b illustrates the degree of lag produced by the thermal protection on the transducers.

The propellant can be extinguished at a predetermined time by releasing the head-end closure of the motor (thereby, depressurizing the combustion chamber) and by purging the combustion chamber with CO_2. The extinguished grains are sectioned and examined for irregular surface regression patterns, such as produced by nonlinear velocity coupling.

2.1.2 Experimental Results

The experiments were planned with two characteristic frequencies of the propellant/motor system in mind: the fundamental longitudinal frequency of the combustion chamber, f_c^*, (between 1900 and 2100 Hz for the 25 cm grains) and the resonant frequency of the pressure-coupled dynamic burning processes, f_b^*. It was anticipated that the strongest coupling between chamber and propellant responses and, thus, the maximum pressure amplitudes would occur when the excitation frequency was equal to f_c^* and when the chamber pressure was selected so that f_b^* equaled f_c^*. The calculated propellant response function (for the baseline propellant) indicated that f_b^* and f_c^* would be reasonably close for chamber pressures near 2 to 3 MPa.

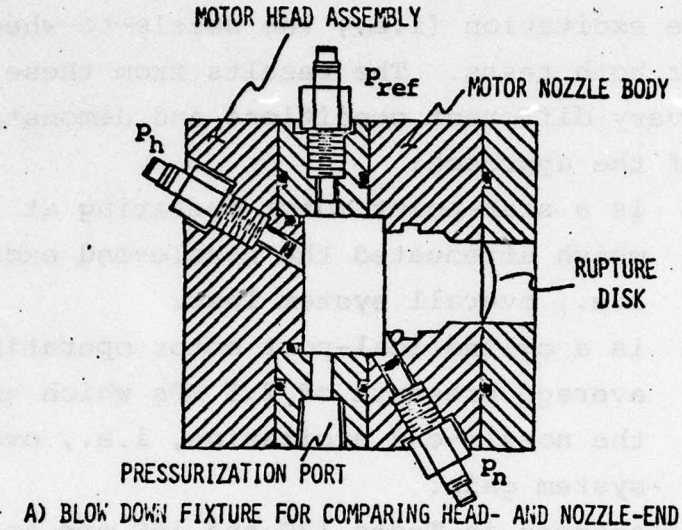

A) BLOW DOWN FIXTURE FOR COMPARING HEAD- AND NOZZLE-END TRANSDUCERS TO REFERENCE PRESSURE TRANSDUCER.

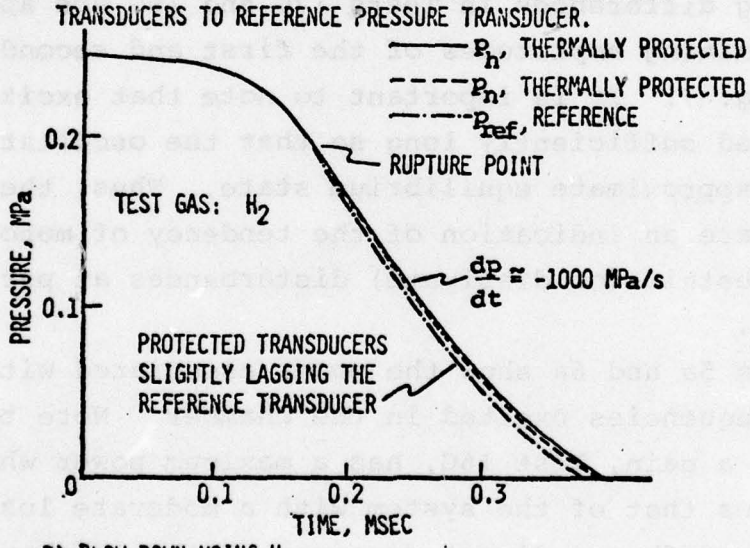

B) BLOW DOWN USING H_2.

Fig. 4 Dynamic calibration of pressure transducers.

Two series of motor firings were conducted: 4 motors for which a range of frequencies were scanned and 6 motor tests at constant frequency. The reduced data for two of the variable frequency tests (17G and 16G) are shown in Figs. 5 and 6. The magnitude of the excitation (i.e., the nozzle-to-wheel spacing) was the same for both tests. The results from these two tests illustrate two very different conditions and demonstrate the effectiveness of the approach:

- o Test 17G is a star-point motor operating at 3.9 MPa which attenuated the nozzle-end excitation, i.e., overall system loss.
- o Test 16G is a cylindrical-port motor operating at an average pressure of 2.5 MPa which amplified the nozzle-end excitation, i.e., overall system gain.

The striking differences in Tests 17G and 16G are apparent from the limiting amplitudes of the first and second harmonics shown on Fig. 7. It is important to note that excitations are sustained sufficiently long so that the oscillations achieve an approximate equilibrium state. Thus, the limiting amplitudes are an indication of the tendency of motor/propellant system to sustain (or dissipate) disturbances at particular frequencies.

Figures 5a and 6a show the power associated with the range of frequencies excited in the chamber. Note that the system with a gain, Test 16G, has a maximum power which is more than 10 times that of the system with a moderate loss, Test 17G. Figures 5b and 6b are direct measures of the relative gains associated with each test after the limiting amplitudes have been achieved. The phase angle between pressure oscillations at two stations is often used in acoustic studies to establish whether a loss or a gain has occurred in a flowing system. When the phase angle is negative, the nozzle-end response leads the head-end response by the indicated absolute value.

Thus, the results of Figs. 5c and 6c are consistent with the gains and limiting amplitudes displayed in the a and b parts of the figures.

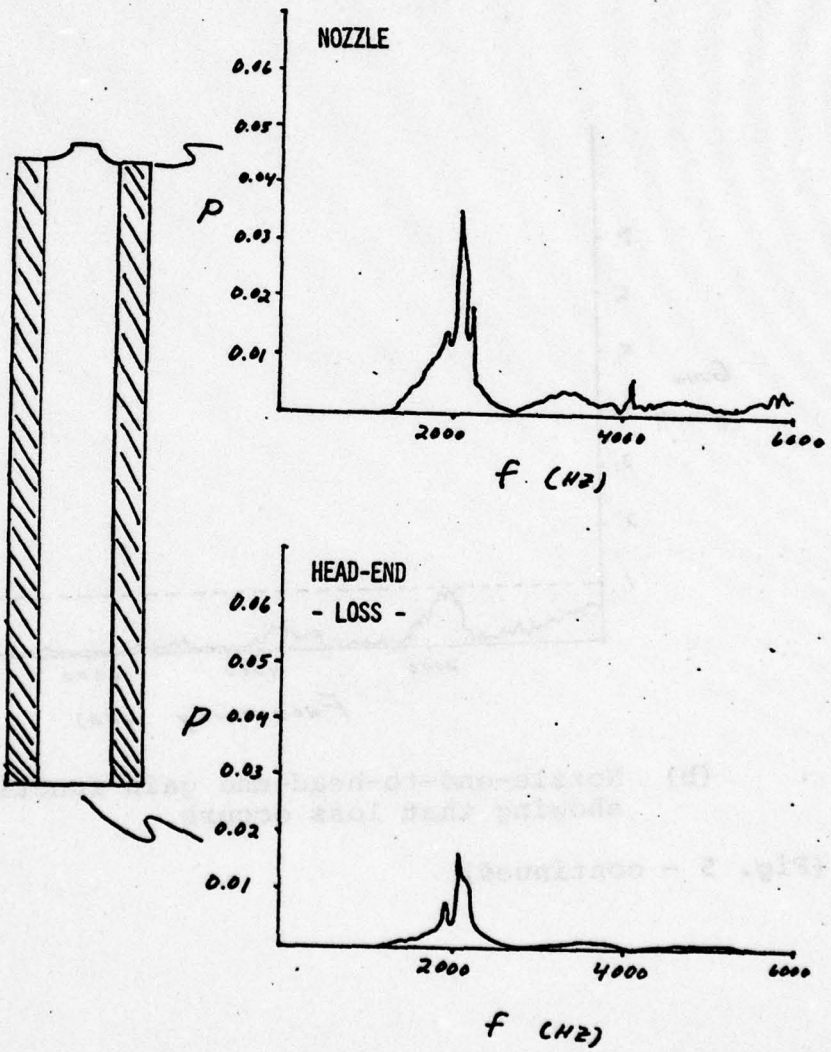

(a) Power at first three harmonics is attenuated between nozzle and head end.

Fig. 5 Nozzle- and head-end power spectra comparing excitation at nozzle end and head end (6-pointed star at 3.9 MPa, Test 17G).

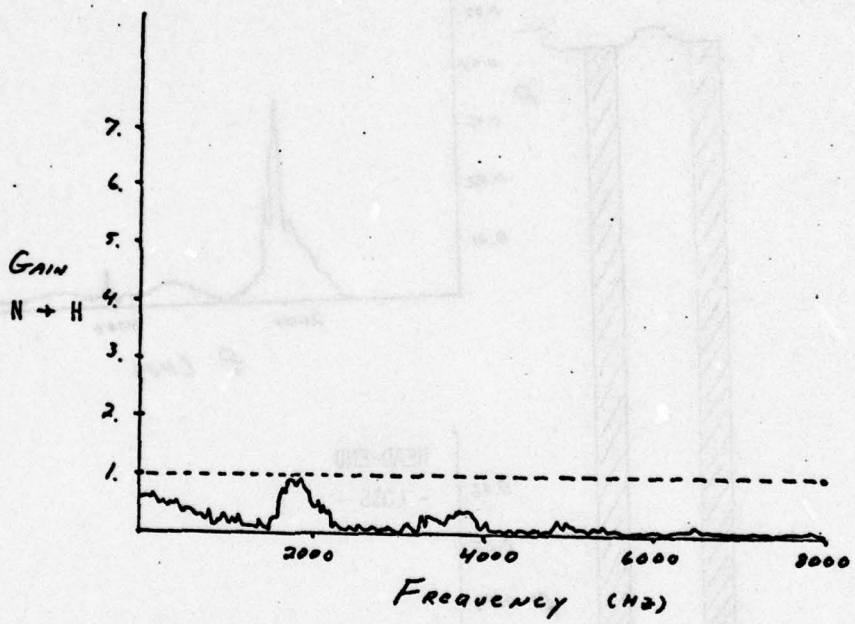

(b) Nozzle-end-to-head-end gain function showing that loss occurs.

(Fig. 5 - continued)

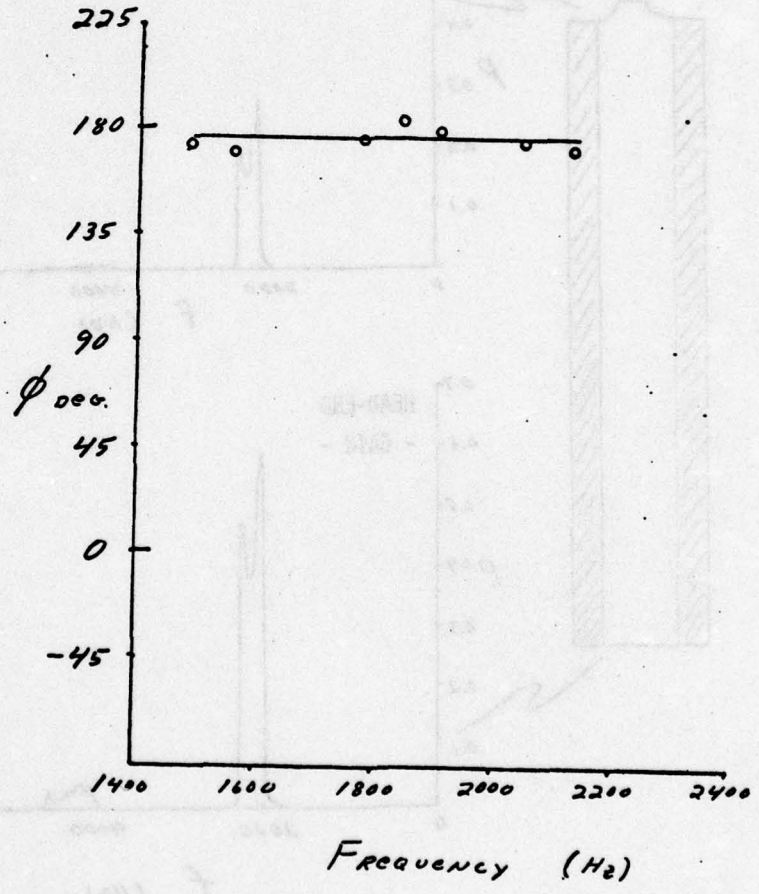

(c) Phase lag from nozzle-end-to-head-end for first harmonic. Phase angle of approximately 180° indicates that losses along port are moderate.

(Fig. 5 - continued)

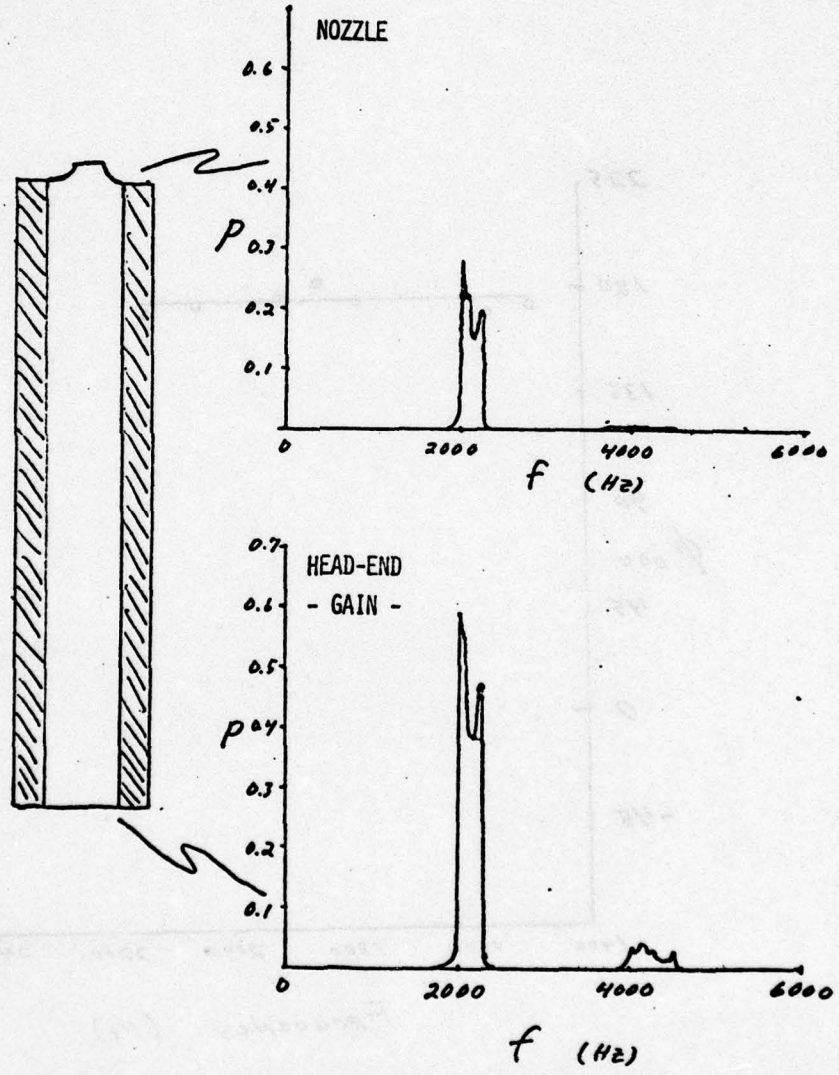

(a) Power at first and second harmonics is amplified between nozzle and head end. Maximum power of first harmonic grows to over 10 times that of Test 17G.

Fig. 6 Nozzle- and head-end power spectra comparing excitation at nozzle end and head end (cylindrical port at 2.5 MPa, Test 16G).

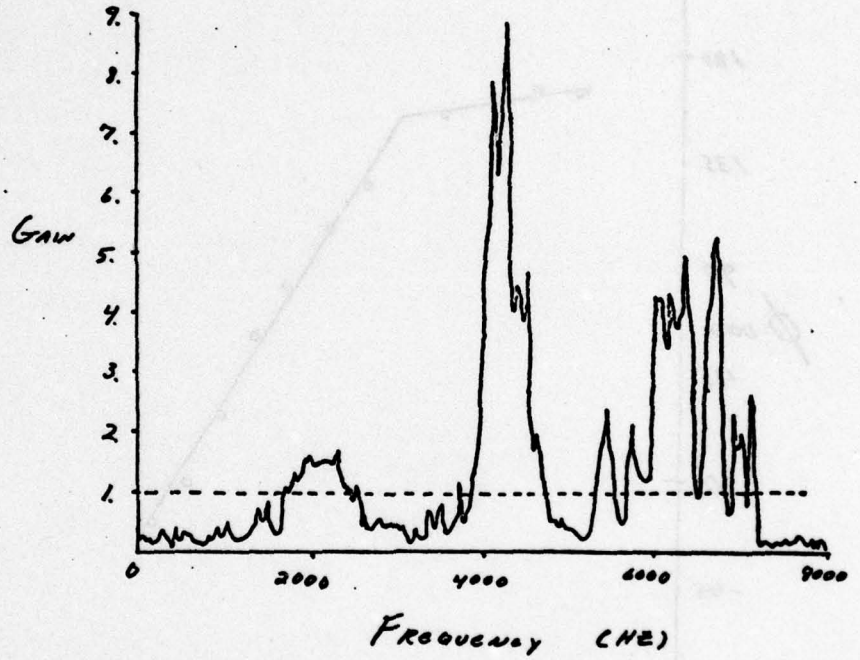

(b) Nozzle-to-head-end gain function showing that gains occur and are most prominent for the second harmonic.

(Fig. 6 - continued)

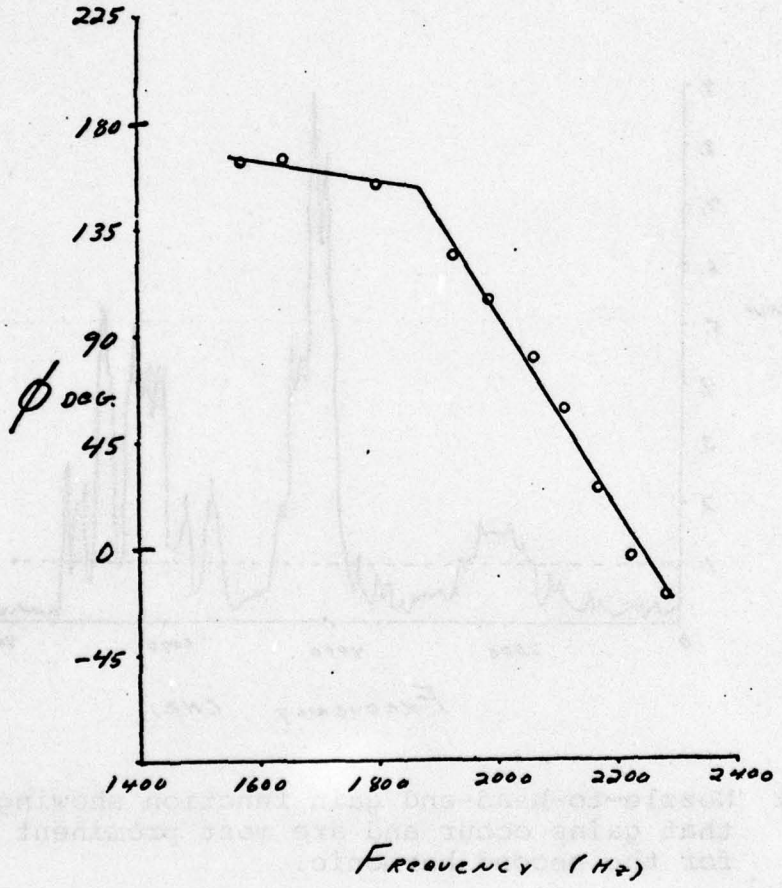

(c) Phase lag from nozzle-end-to-head-end for first harmonic shows that gains occur along the port.

(Fig. 6 - continued)

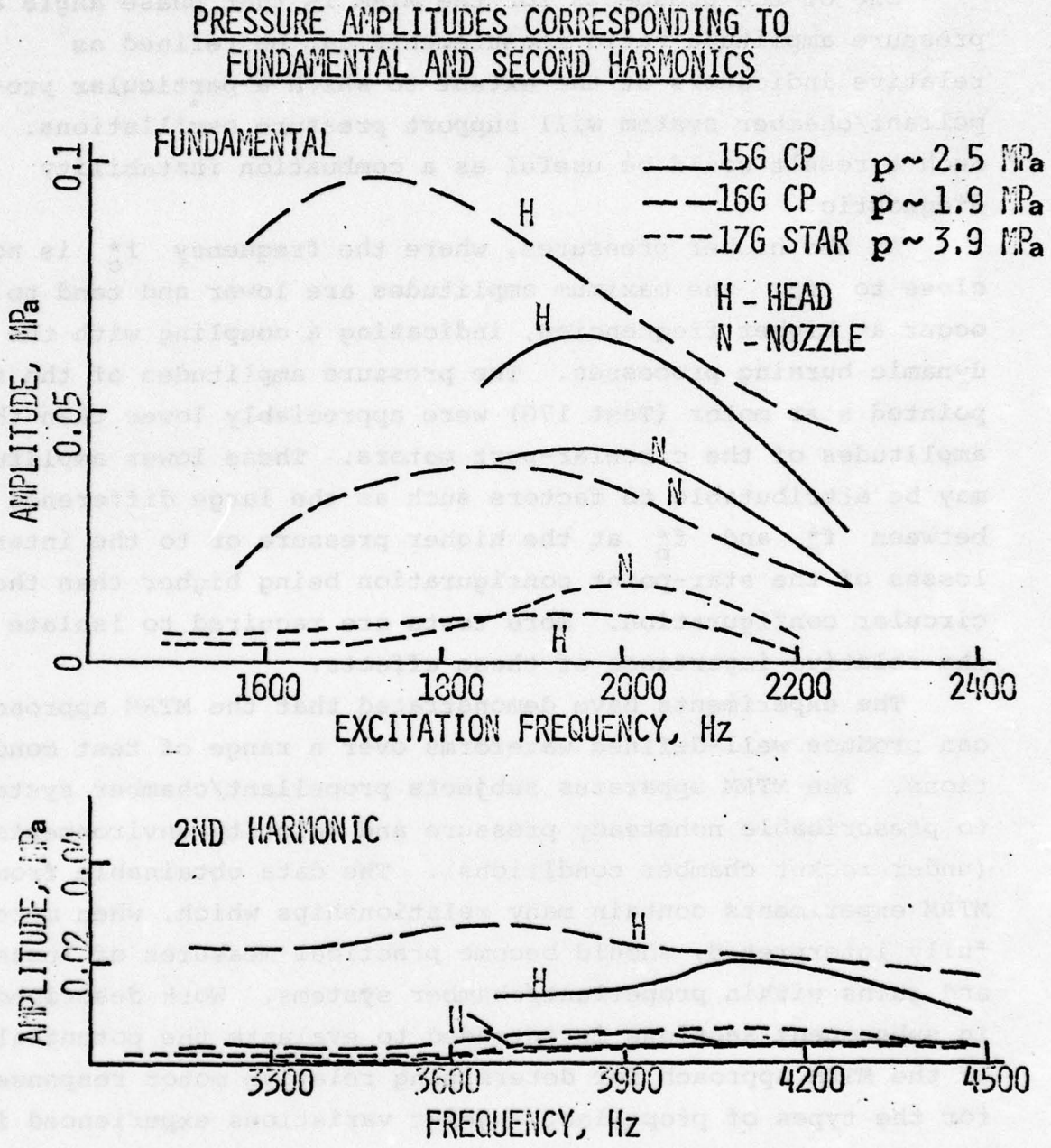

Fig. 7 Pressure amplitudes corresponding to fundamental and second harmonics showing that limiting pressure amplitudes are much higher when gains occur.

One of the prospects for the MTRM is that phase angle and pressure amplitude ratio measurements can be refined as relative indicators of the extent to which a particular propellant/chamber system will support pressure oscillations. Such a result would be useful as a combustion instability diagnostic.

At the higher pressures, where the frequency f_c^* is not close to f_b^*, the maximum amplitudes are lower and tend to occur at higher frequencies, indicating a coupling with the dynamic burning processes. The pressure amplitudes of the six-pointed star motor (Test 17G) were appreciably lower than the amplitudes of the circular-port motors. These lower amplitudes may be attributable to factors such as the large difference between f_c^* and f_b^* at the higher pressure or to the internal losses of the star-point configuration being higher than the circular configuration. More tests are required to isolate the relative importance of these effects.

The experiments have demonstrated that the MTRM approach can produce well-defined waveforms over a range of test conditions. The MTRM apparatus subjects propellant/chamber systems to prescribable nonsteady pressure and velocity environments (under rocket chamber conditions). The data obtainable from MTRM experiments contain many relationships which, when more fully interpreted, should become practical measures of losses and gains within propellant/chamber systems. Work described in subsequent sections is intended to evaluate the potential of the MTRM approach for determining relative motor responses for the types of propellant/chamber variations experienced in practice, e.g., effects of small changes in formulation, effect of initial temperature, and effect of aluminum particle size.

2.1.3 Analysis of Forced Longitudinal Waves in Rocket Motor Chambers

Recent experiments (as described in Ref. 6 and Section 2.1.2) have demonstrated that modulated throat rocket motor (MTRM) experiments and associated data analysis techniques can accurately record and reproduce the pressure versus time

behavior at the head and nozzle ends of a solid propellant rocket motor chamber. The data reduction of the recorded signals consists of determining the amplitudes and phase relationships of the head- and nozzle-end pressure oscillations. A mathematical model of the propellant combustion and rocket chamber flow field is being developed to interpret the physical processes which produced the observed results. The model incorporates a forced pressure oscillation at the nozzle boundary and includes nonlinear pressure and velocity coupling effects. The flow field is modeled by a numerical solution to the partial differential equations for continuity, momentum, and energy.

Similar mathematical models have been formulated previously although none have been used to consider forced oscillations. Culick[7] considered the linear situation of small amplitude, standing longitudinal waves in a solid propellant rocket chamber. Levine and Culick[8] developed a numerical model of nonlinear instability, first with linearized pressure and velocity coupling[8] and later with nonlinear pressure and velocity coupling.[9] In the latter method, the heat conduction equation was solved numerically. However, the heat feedback due to velocity coupling was calculated by an analogy to the linear pressure-coupling response. Kooker and Zinn[10] developed a similar model; however, velocity coupling was not included. A model of combustion instability where the conservation equations were not solved but which included linear pressure and velocity coupling was described by Dehority and Price.[11] Kuentzmann and Lengelle[4] described a finite element approach which is being undertaken to analyze nonlinear pressure- and velocity-coupling responses in solid rocket chambers.

2.1.3.1 Mathematical Model

The gas flow and propellant burning rates in the MTRM were modeled so that the measured nozzle-end pressure-versus-time, $p_{noz}(t)$, can be used as a forcing function (see Fig. 8). The model employs a solution to the partial

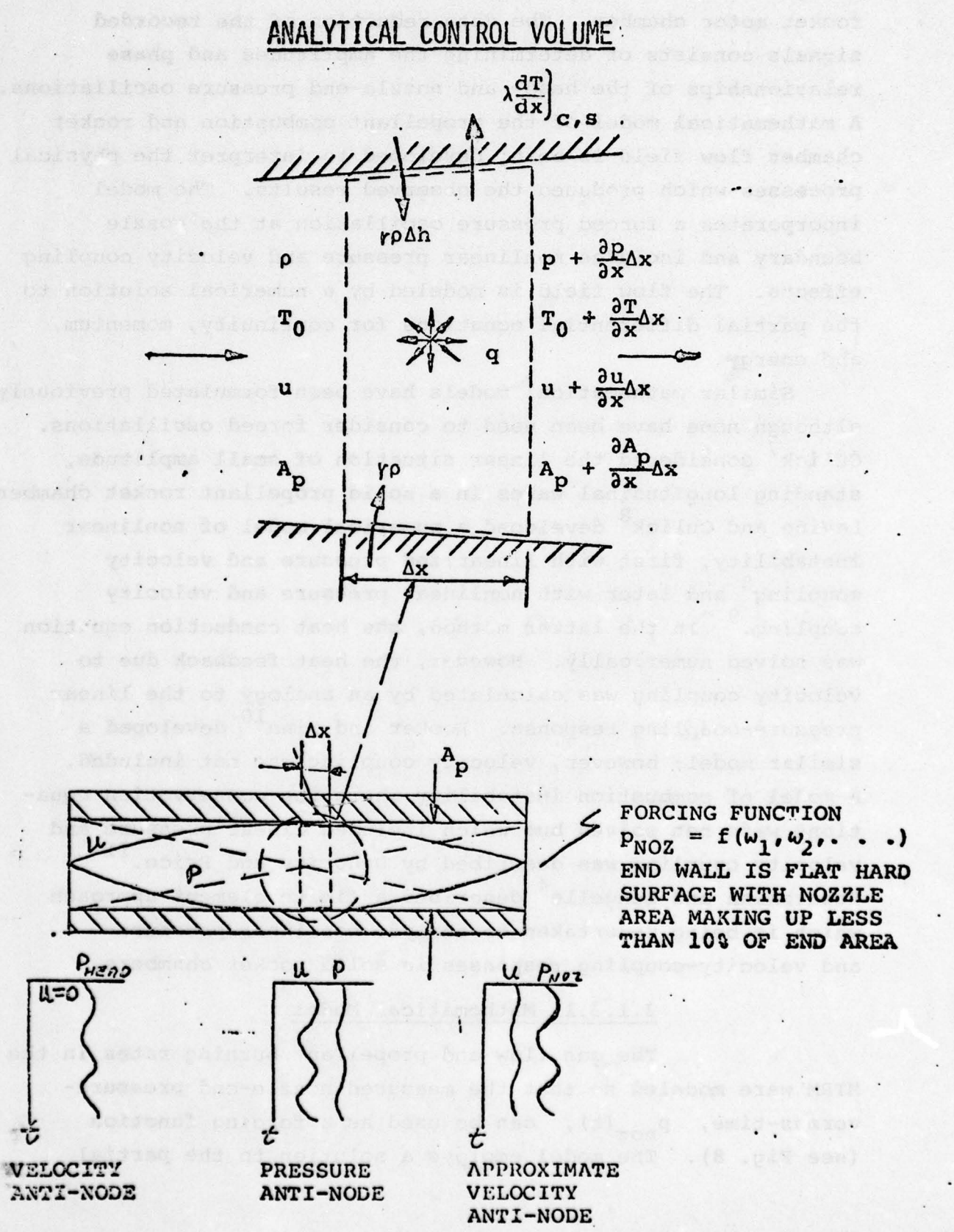

Fig. . 8 Gas dynamic interactions with chamber of

differential equations for energy, continuity, and momentum of the chamber flow coupled to boundary conditions at the gas-stream/propellant interface. Since flow through nozzle is not a consideration in the mathematical formulation, knowledge of how throat area varies with time is not required. The pressure-coupled response is calculated by solving the heat conduction equation at every axial node and using the Zeldovich dynamic burning model.[12] The heat feedback due to velocity coupling is approximated from steady state erosive burning data. The Lenoir-Robillard[13] erosive burning correlation is being used; as improved correlations are developed, they can be incorporated into the model.

The model provides a direct means of testing the validity of candidate methods for calculating the pressure-coupled responses, velocity-coupled responses, and the wave forms in the chamber. In particular, when $p_{noz}(t)\Big|_{meas}$ is imposed, the difference between $p_{head}(t)\Big|_{meas}$ and $p_{noz}(t)\Big|_{calc}$ indicates the degree to which the overall model describes the flow and burning rate responses. The model can be used in the correlation mode by adjusting one or more of the coefficients which are least well defined (e.g., the velocity-coupling surface-blowing coefficient).

Conventional rocket motor performance and stability analyses can be performed using the same computer program that is used to analyze the MTRM. The primary difference is the manner in which the nozzle-end boundary condition is treated. When the MTRM is analyzed, the nozzle-end boundary includes $p_{noz}(t)\Big|_{meas}$ as a forcing formation. When a conventional rocket motor is analyzed, the nozzle-end boundary is the conventional converging-diverging nozzle boundary. Thus, once the experimental data have been correlated, the computer program provides a direct means of calculating motor performance. Of course, there are limitations on the type of motors which can be analyzed. The present form of the program is intended for high length-to-diameter motors which do not have complex grain configurations.

2.1.3.2 Calculated Results

Preliminary results have been obtained from the numerical solution for a sinusoidal pressure excitation at the nozzle end. Figure 9 shows the pressure oscillation versus time at four axial locations in the motor. The excitation frequency is 2000 Hz. The decrease in pressure amplitude from the nozzle end of the port to the head end of the port can be noted along with the increasing phase angle. Figure 10 illustrates pressure versus distance at $\pi/2$ intervals during one oscillation cycle. The existence of two "seminodes" can be seen. These are the result of the interactions between the acoustic waves, the flow field, and the unsteady combustion process. There is no one location where pressure oscillations are zero. Figure 11 shows port Mach number versus distance at the same five time intervals in the cycle. The port Mach number approaches 0.5 at the nozzle end of the chamber. The fluctuation of the velocity is approximately 10% of the mean velocity at the nozzle end of the chamber but increases to above 20% near the center of the port. This indicates that the velocity-coupling contribution to motor instability may be substantial over most of the chamber length.

Figure 12 compares trends calculated using the mathematical model with experimentally measured trends as a function of frequency. The mathematical model (Fig. 12a) shows that the phase lag is proportional to the frequency and that the amplitude of the chamber oscillations, both head and nozzle ends, reach a maximum near 2000 Hz. Figure 12b shows the same trends which were obtained from rocket motor firings.[6] The phase angle increases with frequency.

The head-end and nozzle-end pressure oscillations reach a maximum at approximately 1900 Hz. Work is now in progress to extend the comparisons between the model and experiment.

During the follow-on effort, attention will be focused on the following questions:

1. Are the qualitative calculated trends in agreement with experimental observations.

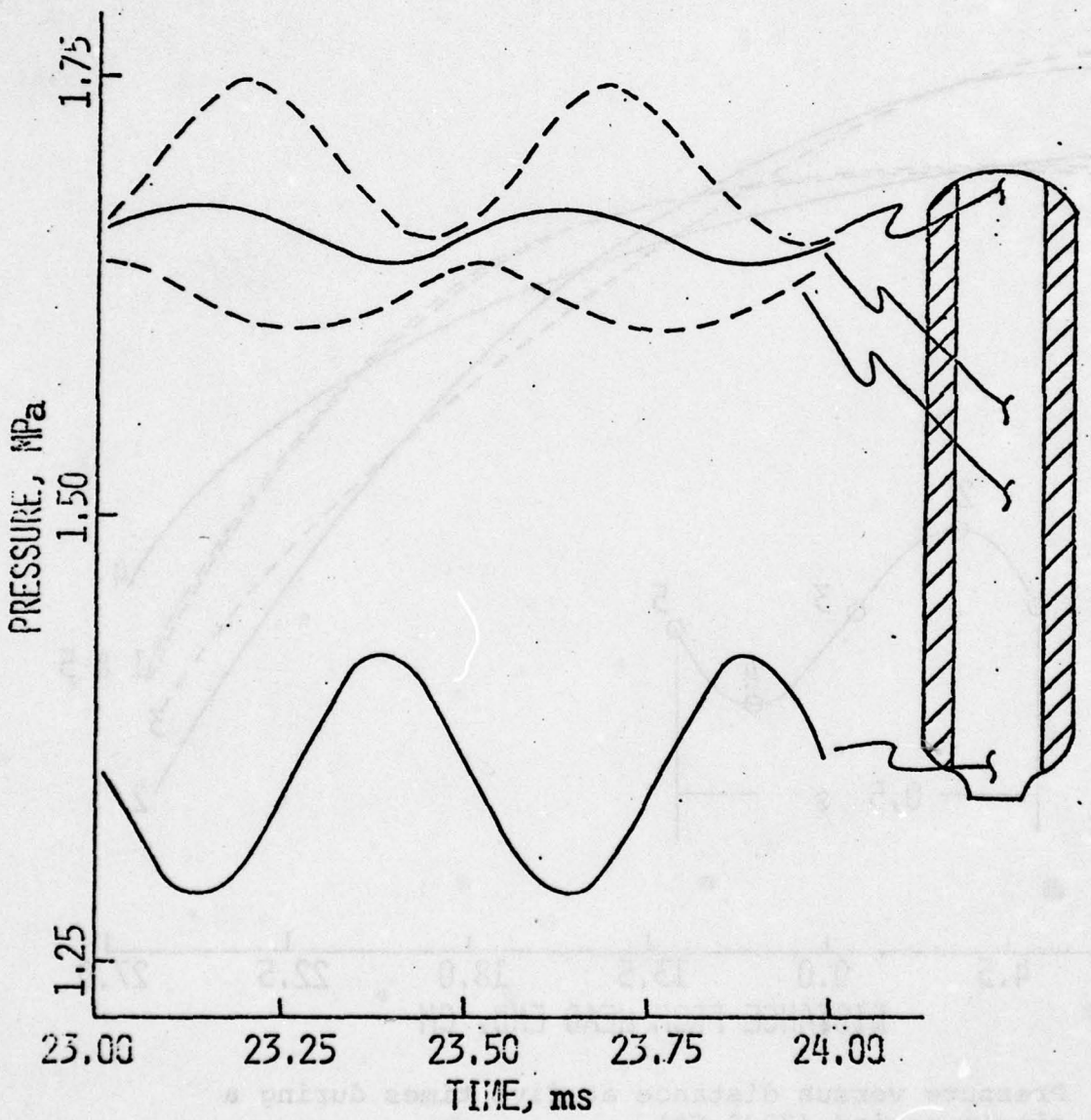

Fig. 9 Pressure versus time at four axial locations. (Excitation frequency is 2000 Hz.)

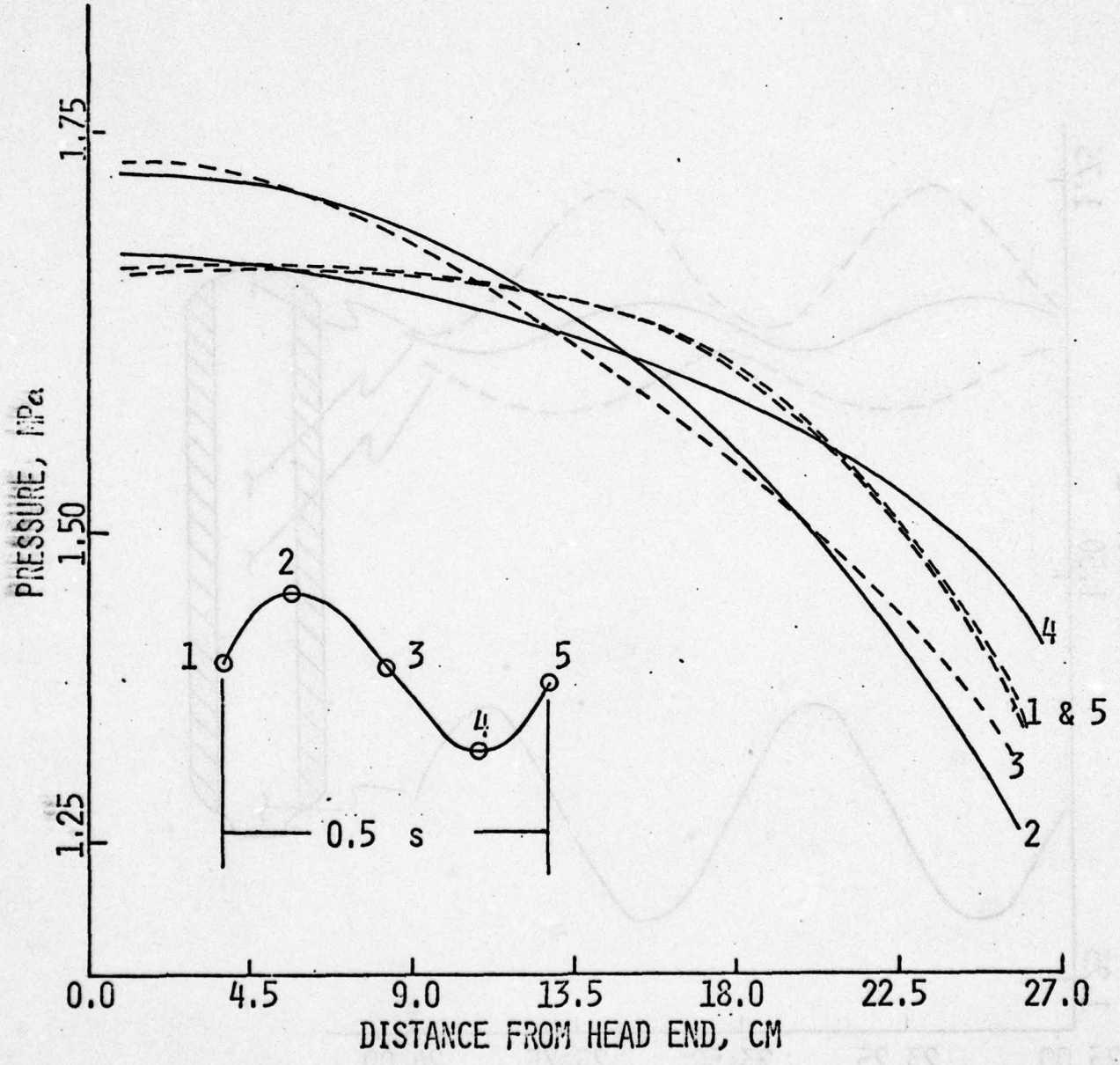

Fig. 10 Pressure versus distance at five times during a single period (2000 Hz).

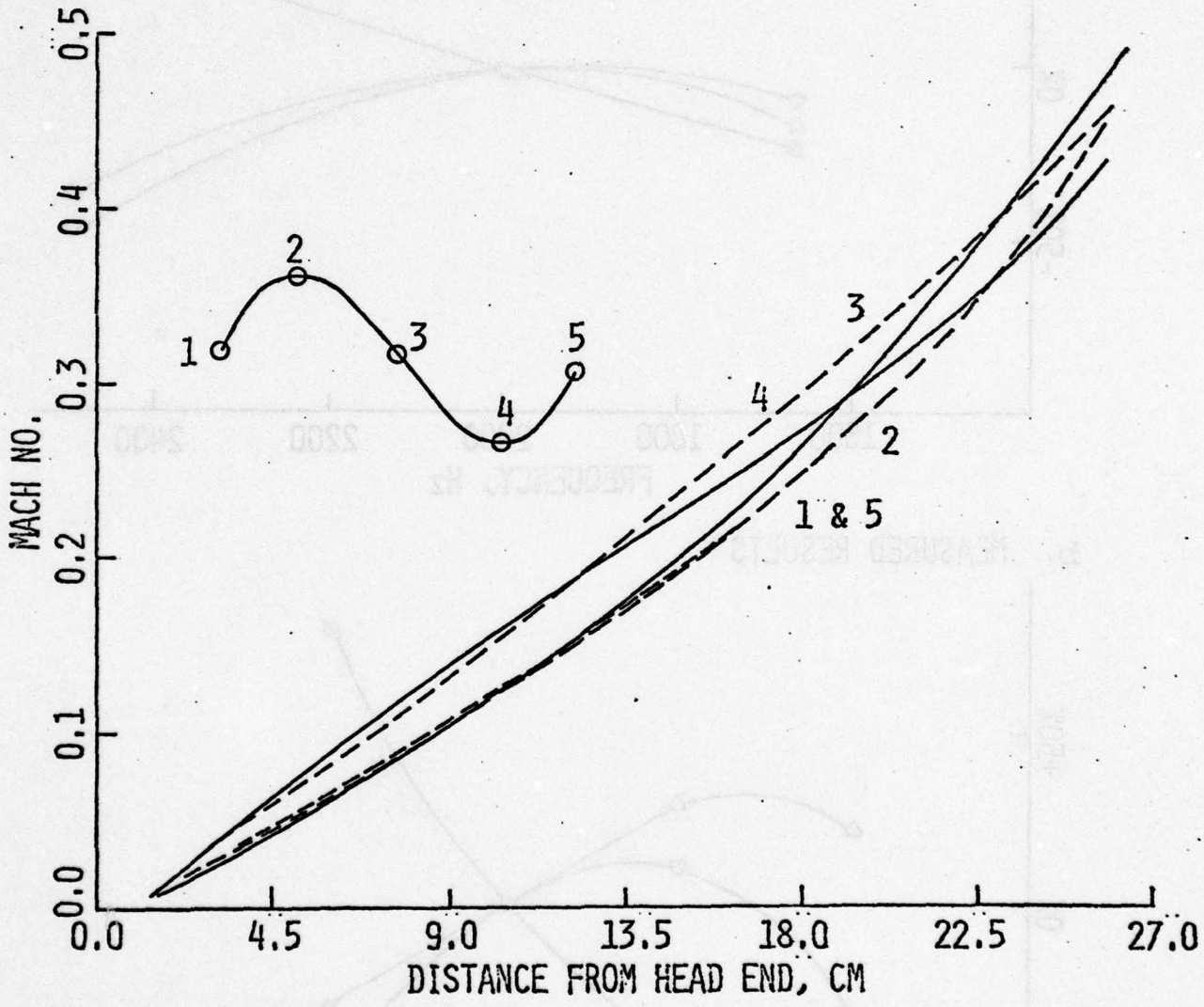

Fig. 11 Mach number versus distance at five times during a single period (2000 Hz).

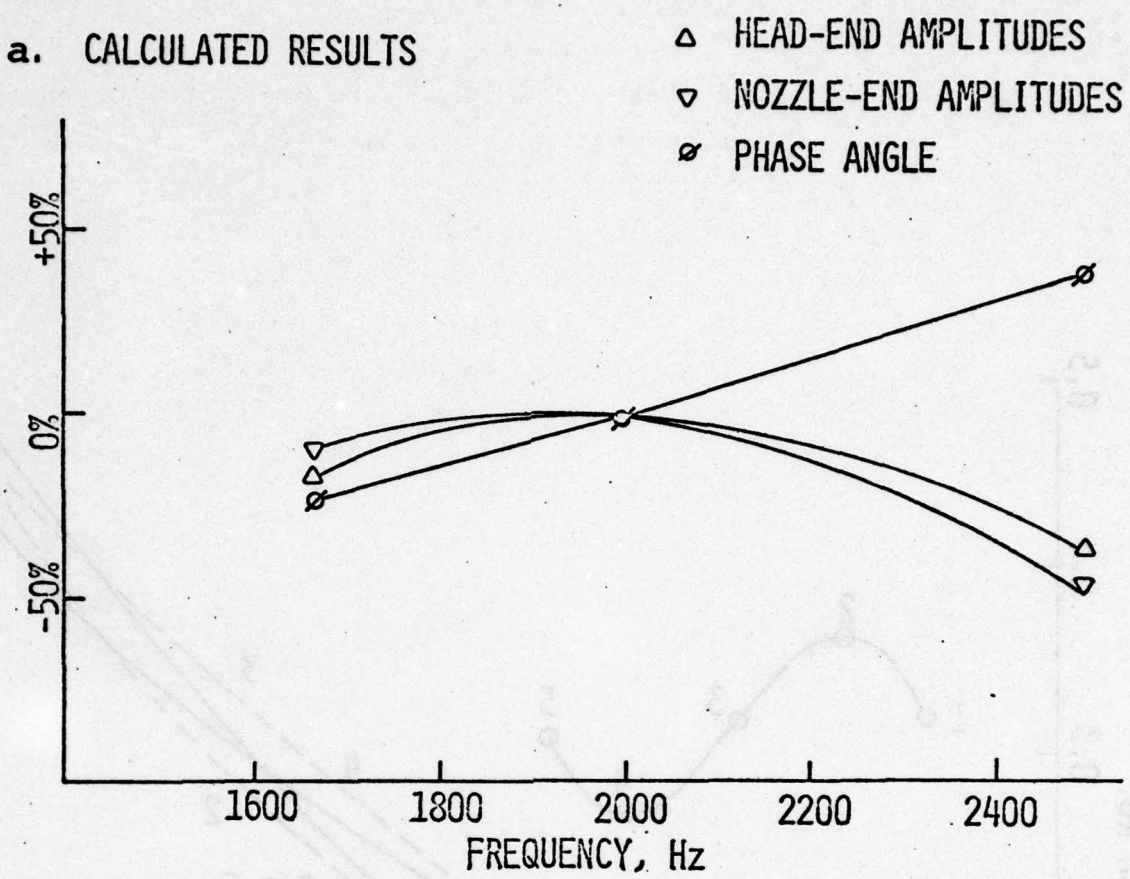

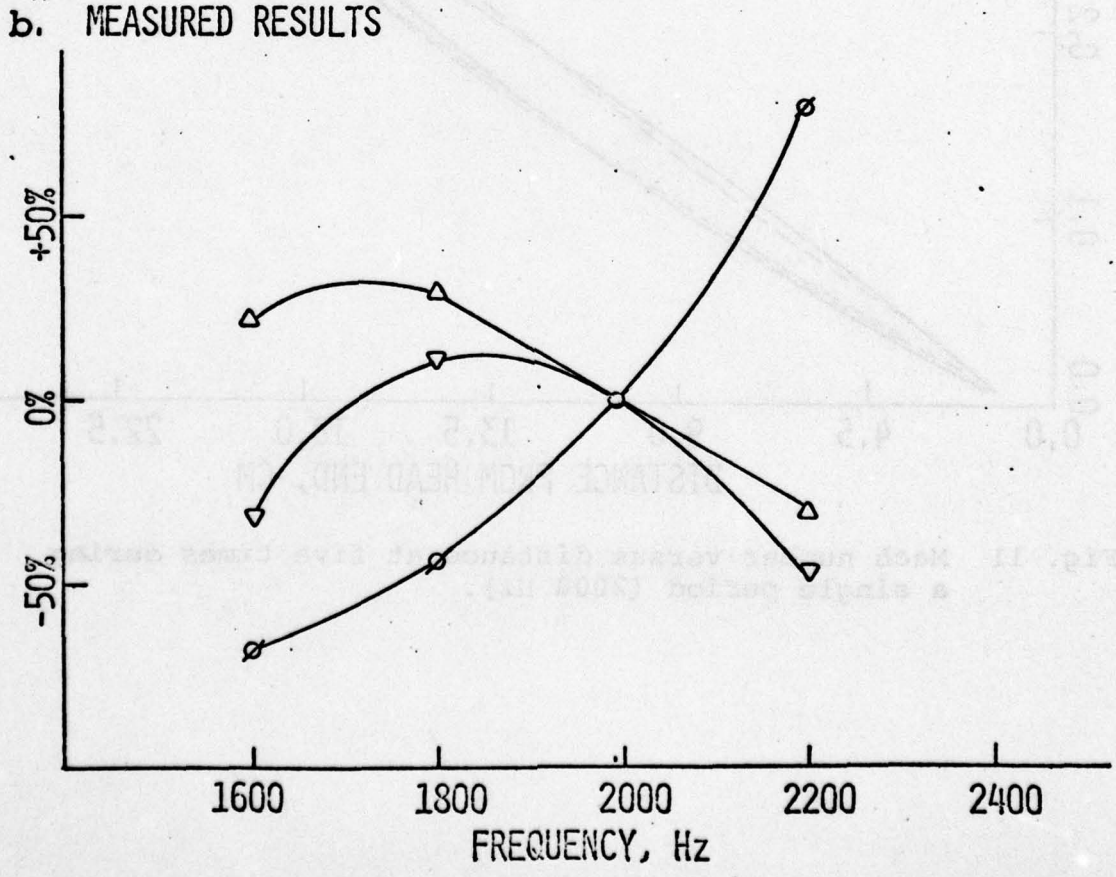

Fig. 12 Percent change in amplitudes and phase angles as a function of frequency.

2. Are the calculated results excessively sensitive to the uncertainties associated with the measured (at other laboratories) propellant response characteristics.
3. Can the experiment distinguish between propellant types, pressure levels, and internal flow conditions.
4. To what extent do the observed correlations permit statements to be made concerning the overall losses or gains that occur along the chamber.

2.1.4 Rocket Motor Experiments

Experiments using the following non-metallized propellant are underway:

1. The base-line propellant:

Binder HTPB%	14.0
Ammonium Perchlorate,%	86.0
20% 15 μm	
40% 45 μm	
40% 180 μm	

The range of test conditions are as follows: pressure varied from 400 to 1200 psi, maximum aft-end Mach numbers up to 0.3, modulation frequency ranging from 1600 to 2500 Hz. In particular, tests are conducted over a range of modulation frequencies, i.e., from 10% greater than the longitudinal frequency to 10% less than the longitudinal frequency.

Two types of grains are used: a cylindrical grain which is progressive and typically produces a 30 to 40% pressure increase during the burn and a six-pointed star grain which produces a nearly neutral (within 10%) pressure trace. The Mach number along the port can be estimated from the p_h and p_n measurements and approximations of port area versus time.

Propellants have been formulated to examine the effects of particulate damping. These AP/HTPB propellants have 86% solids and have the following aluminum particle sizes:

2. 6% Al $\bar{d}_m$ = 50 μm
3. 3% Al $\bar{d}_m$ = 50 μm & 3% Al $\bar{d}_m$ = 15 μm
4. 6% Al $\bar{d}_m$ = 15 μm

Four motors have been manufactured from each of these propellants and will be tested over the next couple of months. Strand burning rate data are presently being obtained for these propellants.

During the follow-on effort a series of smokeless-type propellants with stability additives will be examined. Initially, the following two propellants will be compared to the baseline propellant:

5. Baseline except 1% carbon powder and 13% HTPB.
6. Baseline except 1% ZrC and 13% HTPB.

At the present stage of development, the motor firing data are being examined in terms of the overall chamber/propellant responses. At each frequency range, the data are reduced to the following form:

1. Over the entire burn:
   a. $\Delta p/\bar{p})_h$ & $\Delta p/\bar{p})_n$ vs $M_{max}(t)$
   b. $\Delta p/\bar{p})_h$ & $\Delta p/\bar{p})_n$ vs $p(t)$
2. At prescribed Mach numbers and pressures:
   $\Delta p/\bar{p})_h$ & $\Delta p/\bar{p})_n$
3. Over the entire burn:
   a. Power content at each of the harmonics.
   b. The phase angle and gain (or loss) of Δp_h and Δp_n.

Presenting the data in this manner is giving direct indication of the response of the system. The analytical model is being used to carry out calculations which correspond to each experiment.

2.1.5 Expected Payoff

The expected payoff from the MTRM approach in terms of motor and propellant stability analysis is summarized as:

(1) The modulated throat rocket motor subjects the propellant/chamber combinations to prescribable unsteady pressure and velocity conditions (under rocket chamber conditions). A wide range of p, Δp, v, Δv, L^*, A_p/A_t and characteristic times are obtainable.

(2) The apparatus has the potential for determining the relative motor responses for the types of propellant/chamber variations experienced in practice, e.g., effects of raw material lots, small changes in formulation, effect of initial temperature, aging, etc.

(3) The capability of analyzing the unsteady responses in operational rocket motors is improved, since the complete solution to the continuity, momentum and energy equations (which are being used to analyze and interpret the MTRM data) is being used also to consider unsteady responses in operational rocket motors.

The methods and approaches which are competing with the MTRM approach include: the wealth of T-burner experience, impedance tube methods, pulsed full-scale rocket motors, the dual-vented throat approach, and nonlinear internal ballistics theoretical models.

2.2 Aluminized Solid Propellants Burning in Rocket Motor Flow Field

The emphasis of this portion of the research is on photographing and interpreting the burning of aluminized propellants under the cross-flow conditions that exist in rocket motors. High-speed photographs (up to 4000 frames/sec) are being taken of the aluminum and aluminum oxide agglomerates forming on the surface, the Al/Al_2O_3 agglomerates moving along the surface and entering the flow field, and the Al/Al_2O_3 agglomerates burning (and undergoing further agglomeration) in the flow field. Several laboratories (most notably the work at NWC, e.g., Refs. 14 and 15) have obtained high resolution photographs of aluminized propellants burning as strands in quiescent atmospheres. These photographs revealed a large amount of information about metal burning processes isolated from the shearing forces of high-speed flow. However, to answer the questions that have been raised concerning metal agglomerate particle size and combustion efficiency (e.g., Ref. 16), the results obtained in quiescent atmospheres must be complemented by results obtained under cross-flow conditions. Other investigators[16,17,18] have studied how formulation, pressure, and port geometry affect the size distribution of metal agglomerates under rocket motor conditions, but those investigations were not concerned with visualizing the combustion processes that produced the agglomerates.

2.2.1 Nomenclature for Section 2.2

A_{ex} - particle exposure area
c - aluminum specific heat
d - particle diameter
ℓ - decomposition layer thickness
L - heat of fusion of aluminum
$N_{ag} = t_{ig}/t_{ac,min}$ - criterion for agglomeration
p - pressure
q_s - surface heat flux

r - propellant burning rate

t - characteristic time

α - half angle of exposed surface

$\beta = 6/\pi$ - co-volume coefficient

ϕ - aluminum volume fraction

μ - viscosity

σ - surface tension

Subscripts

ac - accumulation in the decomposition layer

ac,min - minimum accumulation that leads to agglomeration

ig - ignition of aluminum particles

ℓ - mobile decomposition layer

m - melting of aluminum

2.2.2 Experimental Approach

High-speed movies are being taken of aluminized double-base propellants burning in window motors. Figure 13 shows one of the arrangements used to obtain photographs. Typical results from these experiments were explained and interpreted in a recent journal article.[19]

2.2.3 Analysis of Agglomeration and Ignition Processes

The various investigations indicate complex phenomena in which individual aluminum particles accumulate and, under some circumstances, form relatively large agglomerates, each of which contain hundreds or even thousands of original particles. These agglomerates may or may not ignite on the propellant surface.

It was found that any situation in which large amounts of aluminum particles are brought into close contact and maintained under appropriate heating conditions results in the agglomeration of the particles. Particles heated in ovens, e.g., Refs. 20 and 21, as well as those included in solid propellants, experience similar agglomeration processes. An adhesion process starts at a temperature of about 700 K, below the aluminum

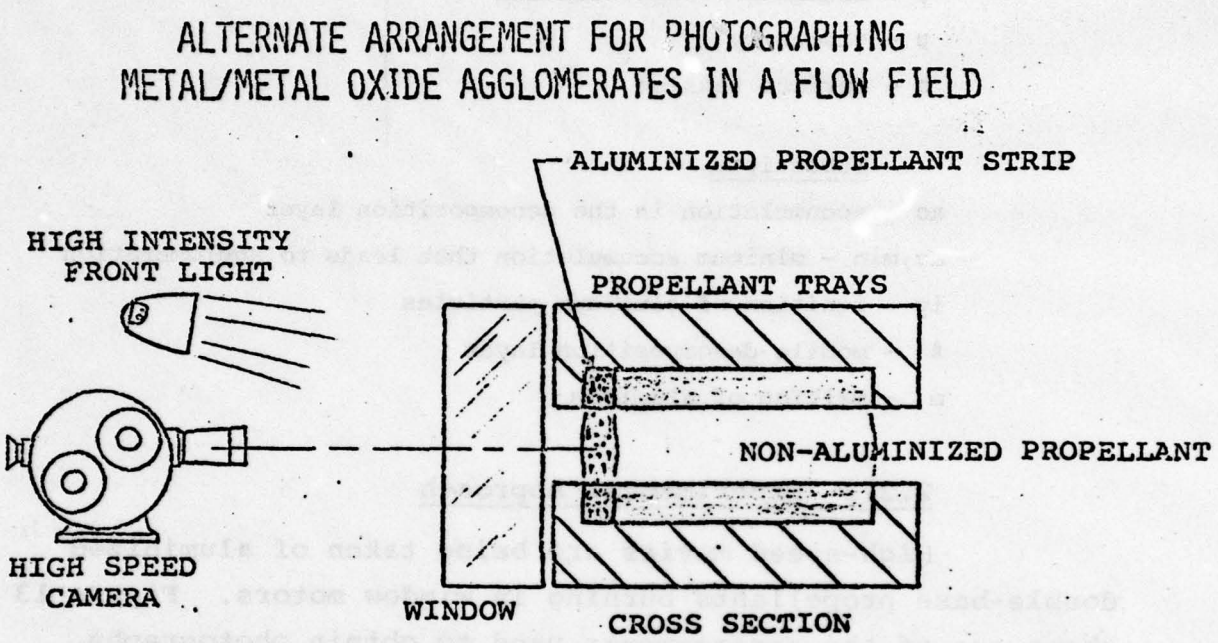

Fig. 13 An alternate arrangement for concentrating the aluminum burning in a narrow range.

melting point. In this stage, the particles remain in their original shape and adhere to one another in an undefined way. At the aluminum melting temperature (933 K), the adhesion process is enhanced by the formation of "welding bridges" among the particles, consisting of molten aluminum flowing through cracks in the oxide shells. The oxide shells remain solid and provide protection against fast oxidation and self-sustained combustion of the particles. According to Pokhil, et al,[17] ignition takes place when the particles achieve the temperature of about 1500 K. Merging of the adjacent particles is accomplished when they reach the Al_2O_3 melting point (2300 K). Then, large agglomerates with spherical shapes are formed.

Previous efforts have explained some of the situations leading to the observed processes of the particle agglomeration, ignition, combustion, and surface ejection. Those investigations are mainly concerned with giving a general explanation of the agglomerate size in composite solid propellants (e.g., Refs. 14 and 18) or the characteristic combustion rates and burning times of the agglomerates in the gas stream.[17]

This study is directed at unifying the observations which have been made concerning the agglomeration mechanism, the ignition processes, and ejection. The propellants which are of interest in this study are those in which the condensed phase granularity is generally less than that of the aluminum particles. The characteristic times of each stage and the forces acting on the particles and their relative importance are evaluated. The effects of burning rate, chamber pressure, surface and gas temperatures, configuration and orientation of propellant, cross-flow, and particle size on the various phenomena are shown and are used to interpret the tendencies obtained in experiments.

The contributions made by other investigators in obtaining experimental data and in interpreting the behavior dependence on various parameters are being used extensively in this study.

2.2.4 Outline of the Physical Model

While the overall combustion process of the propellant appears to be steady, the processes associated with the micro-scale are very unsteady. The model which considers the scale of the individual aluminum particle can be summarized as follows:

1. A thin mobile layer which consists of intermediate decomposition and melt products (referred to as the decomposition layer) exists at the surface. This layer is the site of several processes.
2. Initial heating, and, in some cases, accumulation of the particles takes place in the decomposition layer.
3. Before merging, individual particles are heated separately. Individual particles exposed to intense heating will ignite first.
4. Agglomeration requires a certain minimum of particle accumulation (and close contact) prior to ignition and/or ejection from the surface.
5. Agglomerate size is related to the amount of accumulation before ignition or ejection.
6. Whether agglomeration and/or ignition of particles will take place on the surface depends on the relationship between the characteristic times of accumulation and ignition and on forces acting on the particles.

2.2.4.1 Processes in the Decomposition Layer

The first heating and, in some situations, accumulation of the metal particles can take place in the surface decomposition layer, where the effects of the outer flow are minor. The decomposition layer thickness can be approximated from the solution of the heat conduction equation in the condensed phase. Use was made of data for NC double-base propellant.[19]

The conditions for accumulation in the decomposition layer are the following: (1) the particles are smaller than the decomposition layer thickness, (2) the surface tension overcomes

the forces acting against it (e.g., drag), and (3) either no ignition or delayed ignition of the particles in the decomposition layer occurs. The condition for retaining an individual particle in the decomposition layer (condition 2) is obtained from the balance between the surface tension force and the drag force resulting from the penetration of the retained particle into the decomposition zone at a speed equal to the burning rate, r, (see Fig. 14):

$$\sin^2\alpha = 3\mu_\ell r/\sigma_\ell \tag{1}$$

Calculations based on typical values of μ_ℓ and σ_ℓ reveal that this condition is usually satisfied.

Due to the surface tension, the regressing surface will retain particles as the surface regresses, while only the top of each particle may be exposed to the gas environment. Moving with the regressing surface, each particle will encounter other particles; this process forms a dense packing of particles in the decomposition layer. Additional accumulation will result in the forcing of the accumulate into the gaseous flame zone (see Fig. 15).

The characteristic accumulation time in the mobile decomposition layer, t_{ac}, is defined as the time required to fill the decomposition layer with metal particles,

$$t_{ac} = \ell/\beta\phi r \tag{2}$$

Characteristic heating times for the beginning of aluminum melting, t_m, and particle ignition, t_{ig}, in the decomposition layer can be approximated on the basis of heat flux data and exposed area. The exposed area for heating can be found from the forces balance

$$A_{ex} = \pi d^2 \sin^2\alpha/4 = 3\pi\mu_\ell r d^2/4\sigma \tag{3}$$

Hence, the heating times are:

$$t_m \cong \frac{2}{9}\frac{d\rho c\Delta T_m \sigma}{q_s \mu_\ell r} \tag{4}$$

$$t_{ig} \cong \frac{2}{9} \frac{d\rho(c\Delta T_{ig} + L)\sigma}{q_s \mu_\ell r}$$

where ΔT_m and ΔT_{ig} are the temperature elevations needed to achieve the melting and ignition temperatures, respectively.

2.2.4.2 Surface Processes

Heating and flow effects are much more intense above the surface than in the decomposition layer. Final agglomerate size, ignition process, and ejection from the surface are all affected by the conditions on the surface. When accumulates (or particles) are protruding from the condensed phase, their leading edge is fully exposed to surface heat flux conditions. The characteristic times for melting and ignition become much shorter than when they are in the decomposition layer. When the particles on the top of the accumulate ignite and flame spreads over the accumulate, additional heat is provided for melting and merging of the particles, and a larger burning agglomerate may be formed.

A condition for minimum accumulation that can lead to agglomeration is taken as an accumulation of one densely-packed particle layer. Hence, characteritic time for minimum accumulation is

$$t_{ac,min} = d/\beta\phi r \qquad (6)$$

2.2.5 Observations Based on the Proposed Model

The proposed model provides a means to examine the behavior of aluminum in double-base or other homogeneous propellants. A complex dependence of surface processes on various factors can be drawn. Different effects can be interpreted by the relationship among the various characteristic times. The potential of the model will be demonstrated in this summary by the examination of a few parameters. Other factors are being treated in similar fashion and are included in the technical papers.

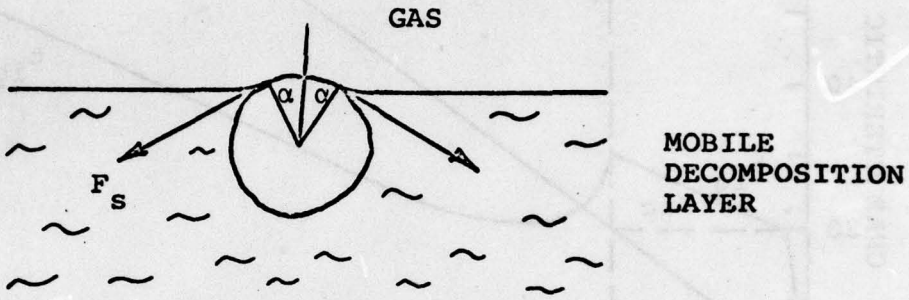

Retaining of metal particle in the decomposition layer by the surface tension force.

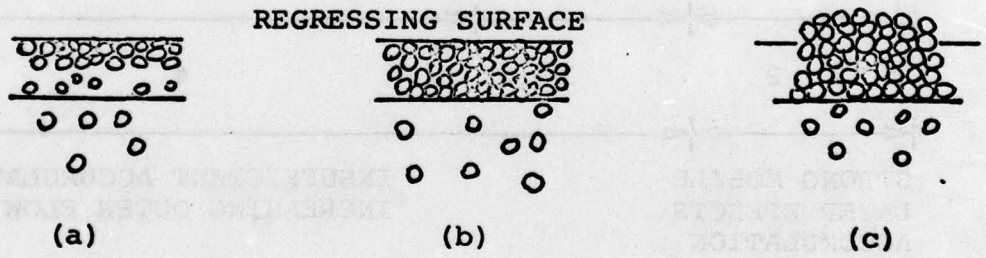

Fig. 14 Accumulation process in the decomposition layer: (a) decomposition layer is partly filled; (b) decomposition layer full; (c) accumulate forced into gaseous flame zone.

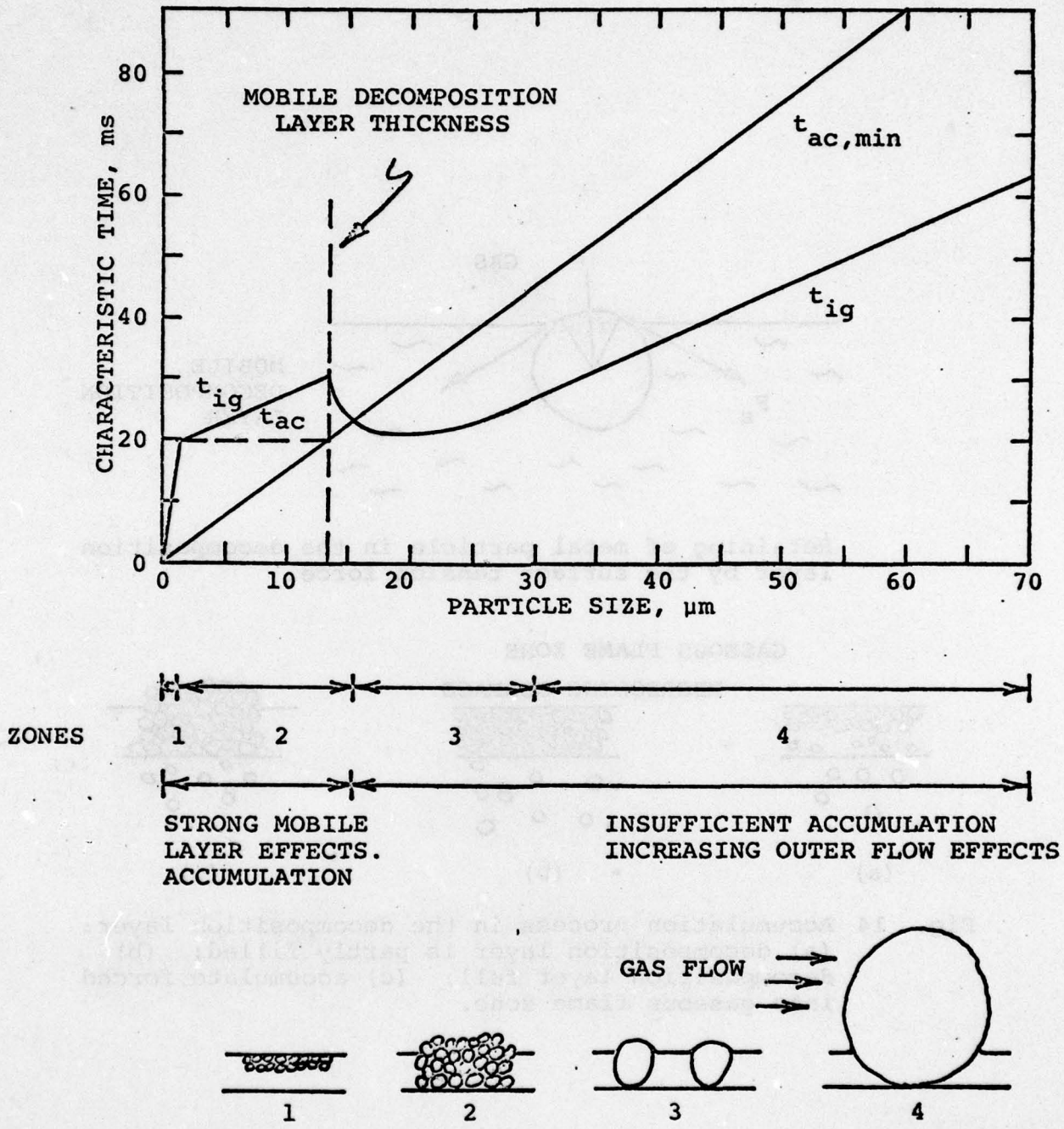

Fig. 15 Characteristic times of accumulation and ignition of aluminum particles.

Figure 15 shows the dependence of agglomeration, ignition, and ejection processes on the aluminum particle size. This figure was drawn for an NC propellant which contains 13% of aluminum at 3.8 MPa (550 psi). It demonstrates the domains in which the particle behavior is changed from agglomeration and ignition on the surface to ejection of unignited individual particles. Such maps can be plotted for different pressure and aluminum content values to show how these factors affect the various processes. Although systematic evidence for this behavior is not available over a broad range of propellants, experimental data in agreement with Fig. 15 exist for limiting cases (zones 2 and 4 in Fig. 15).[17,19]

According to the outline of the model, agglomeration will not take place if individual particles ignite prior to sufficient accumulation. Applying this statement to particles smaller than the decomposition layer thickness, a nondimensional number

$$N_{ag} \equiv t_{ig}/t_{ac,min} \tag{7}$$

can be used as a criterion for agglomeration. Agglomeration degree will increase for $N_{ag} > 1$ and decrease (sharply) for $N_{ag} < 1$. It was found (see Eqs. 5 through 7) that

$$N_{ag} \propto \phi/q_s \tag{8}$$

Thus, at higher surface heating (higher pressure) a higher percent of aluminum may be required to assure agglomeration.

The Fig. 16 results demonstrate clearly the very important concept of decreasing agglomerate size with increasing particle size in the vicinity of N_{ag} of unity. High-speed motion pictures reveal that particles with diameters as large as approximately two reaction layer thicknesses ignite on the surface (both when forming agglomerates and when burning individually). In the 2 to 10 MPa pressure range, particles larger that 40 μm tend to ignite several millimeters above the surface in the flame zone.

Figure 17 illustrates the agreement between the calculated and experimental results as a function of particle size and pressure.

The model explains the known trend of decreasing average agglomerate size with increasing pressure. The reduction in reaction layer thickness with increasing pressure leads to a smaller degree of accumulation and, thus, smaller agglomerates. Other factors such as increased surface heating rate with increased pressure lead to more rapid ignition and, thus, shorter stay times on the surface at higher pressures. The four agglomeration and ignition zones described in Fig. 15 shift toward smaller particle sizes as pressure increases. Thus, smaller particles are necessary for agglomeration at higher pressures.

a) Al PARTICLE SIZE ∿ 6 μm.

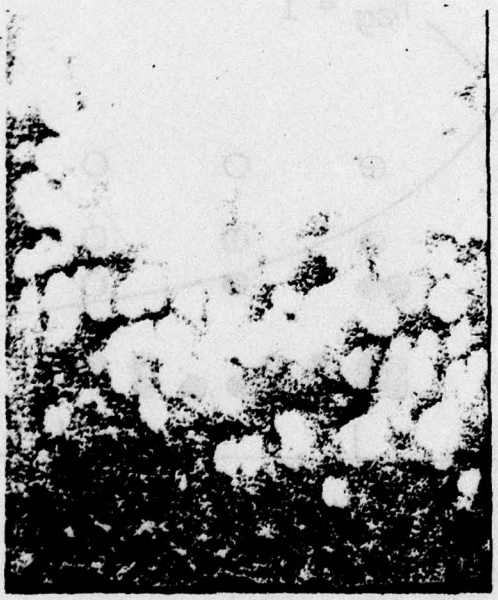

b) Al PARTICLE SIZE ∿ 12 μm.

Fig. 16 Photographs of burning aluminum particles and agglomerates ejected from the propellant surface showing that agglomeration is more prominent for smaller particles (7.6 MPa).

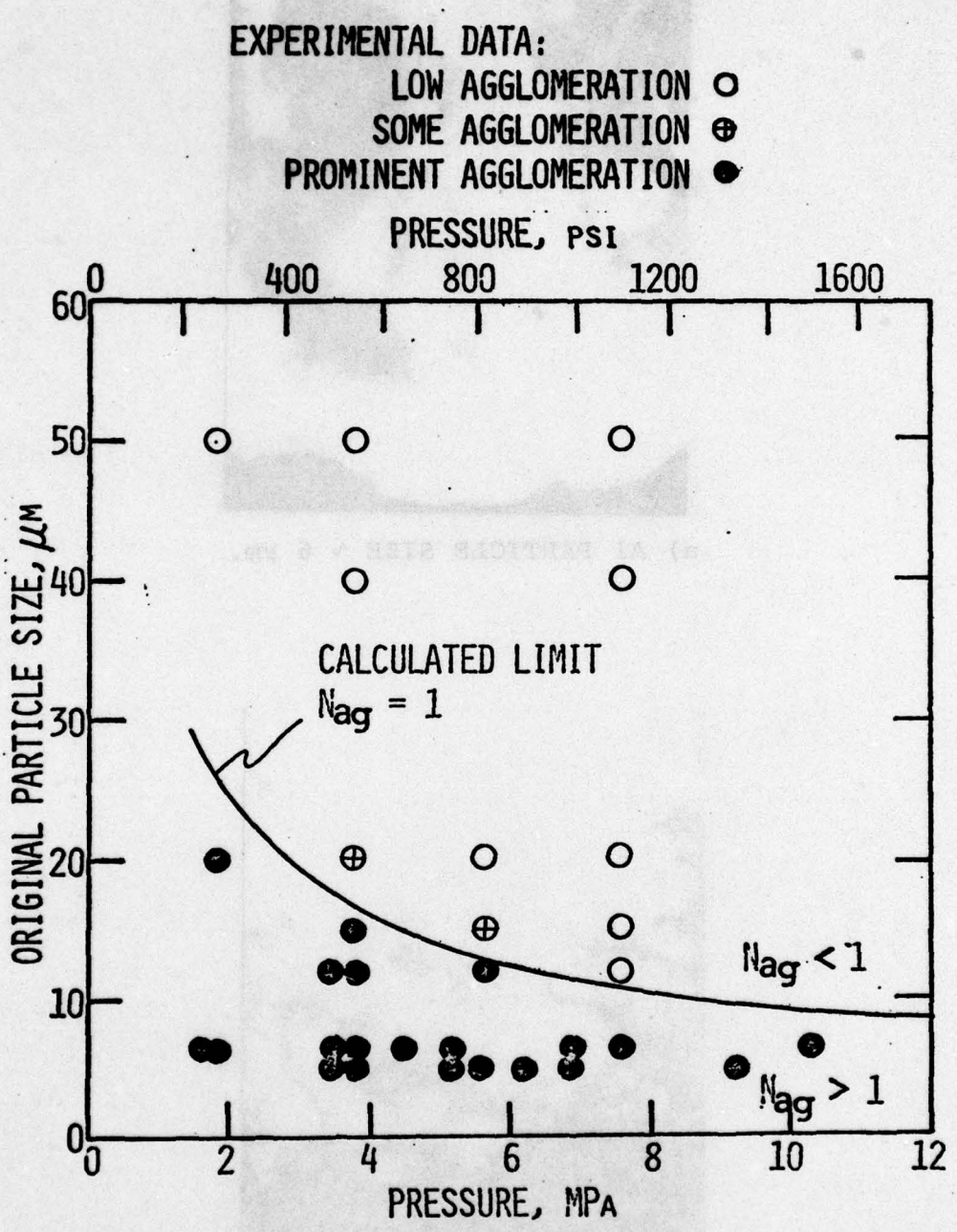

Fig. 17 Agglomeration as a function of particle size and pressure.

2.2.6 Aluminized Propellant Experiments

The experimental techniques were developed using aluminized double base propellants. Recently, methods of photographing high loading density (88 - 89% solids) AP composite propellants have been explored. The results are encouraging and it is believed that during the continuation studies the flow processes adjacent to the burning surface can be visualized. During the continuation studies, emphasis will be placed on obtaining data for:

- o 88 to 90% solids AP propellants with 18 to 20% Al
- o 88 to 90% solids AP/HMX propellants with 18 to 20% Al

The data will be obtained in the 3 to 10 MPa (450 to 1500 psi) pressure range and at cross-flow velocities approaching 100 m/s.

The data base for the aluminized double base propellants will be broadened to explore how agglomerate size varies with Al percentage and Al particle size.

2.2.7 Expected Payoff

Knowledge of Al/Al_2O_3 agglomerate size is of fundamental importance to the application of aluminized solid propellants. Since aluminum is added to increase specific impulse, its effectiveness depends on maximizing its completeness of combustion prior to its ejection from the exit plane. Recent studies at AFRPL[16] have shown that major performance losses are relatable to the combustion inefficiency of aluminum. An improved understanding of those factors that influence agglomerate size may permit propellant/motor chamber designs which produce agglomerates that burn more completely. The effectiveness of agglomerates as dissipators of acoustic energy depends on their particle size distribution, i.e., the smaller agglomerates are more effective for the higher frequencies and vice versa. Naturally, the ability to influence agglomerate size in a systematic manner is of primary importance in defeating combustion instability.

The experimental/analytical methodology offers the prospect of being able to predict the diameter range of the aluminum fuel that will tend to produce a particular range of agglomerate

sizes. For example, near the cross-over point of the ignition and agglomerate characteristic time lines, the agglomerate size tends to be that produced by burning a single aluminum particle. Thus, larger agglomerates can be achieved by using aluminum particles which are either significantly smaller or larger than the particle size at the cross-over point.

2.2.8 Conclusions Pertaining to Aluminum Agglomeration

The model which treats the accumulation of the aluminum particles in the mobile reaction layer adjacent to the burning surface and retention of particles by surface tension forces interprets experimental findings and categorizes agglomeration and particle behavior regimes as follows: (1) Decrease of agglomerate size with increasing pressure, (2) Agglomeration limits as a function of aluminum content (different limits for small and large aluminum particles), and (3) Two main agglomeration and ignition regimes with respect to particle size: (a) Prominent agglomeration (and ignition at the surface) for small particles (up to the order of one reaction layer thickness), and (b) sharply reduced agglomeration degree for larger particles.

The results of this study provide a framework for interpreting how agglomerate size is affected by aluminum particle sizes and mass fraction. The interpretations can be used as a basis for selecting an aluminum particle size (for a given pressure burning rate and aluminum loading) which will tend to give the minimum agglomerate size.

3.0 PUBLICATIONS, PRESENTATIONS, AND PROFESSIONAL PERSONNEL

3.1 Publications and Presentations

The following publications were prepared:

"Aluminized Solid Propellants Burning in a Rocket Motor Flow Field," AIAA Journal, Vol. 16, No. 7, July 1978, pp. 736-739. A. Gany, L. H. Caveny, and M. Summerfield.

"Solid Propellant Rocket Motor Responses Evaluated by Means of Forced Longitudinal Waves," AIAA Paper 77-974, AIAA, New York, NY, July 1977. M. M. Micci, L. H. Caveny, and M. Summerfield.

"Flow Field Effects on Combustion of Aluminized Propellants," Proceedings of the 14th JANNAF Combustion Meeting, August 1977, CPIA Publ. 292, Vol. I, pp. 235-242. L. H. Caveny, A. Gany, and M. Summerfield.

"Agglomeration and Ignition Mechanisms of Aluminum Particles in Solid Propellants," to be published in Proceedings of 17th International Symposium on Combustion, August 1978. A. Gany and L. H. Caveny

The following papers have been accepted for presentation:

"Breakup of Al/Al_2O_3 Agglomerates in Accelerating Flow Fields," accepted for presentation at the 17th AIAA Aerospace Sciences Meeting, January 1979. L. H. Caveny and A. Gany.

"Aluminum Combustion Under Rocket Motor Conditions," accepted for presentation at the AGARD/PEP 53rd Meeting, 2-6 April 1979. L. H. Caveny.

An abstract of the following paper has been submitted:

"Linear Analysis of Forced Longitudinal Waves in Rocket Motor Chambers," submitted to AIAA 15th Propulsion Conference to be held June 18-20, 1979. M. M. Micci, L. H. Caveny. W. A. Sirignano.

3.2 Professional Personnel Associated with Research Effort

The professional personnel associated with the research effort were: L. H. Caveny, M. Summerfield, W. A. Sirignano, A. Gany, and M. M. Micci.

REFERENCES

1. Brown, R. S., Erickson, J. E. and Babcock, W. R., "Combustion Response Function Measurement by the Rotating Valve Method," AIAA Journal, Vol. 12, No. 11, November 1974, pp. 1502-1510.

2. Brown, R. S., "Further Development of the Rotating Valve for Combustion Response Measurements," Proceedings of 12th JANNAF Combustion Meeting, CPIA Publ. 273, Vol. II, December 1975, pp. 65-82.

3. Barrere, M., and Nadaud, L., "ONERA and SNPE Recent Work on Solid Propellant Combustion Instability," J. Spacecraft, Vol. 11, No. 1, January 1974, pp. 33-40.

4. Kuentzmann, P. and Lengelle, G., "Recent Activity at ONERA on Combustion Instability and Erosive Burning," 1977 AFOSR/AFRPL Rocket Propulsion Meeting, Lancaster, CA, March 1977.

5. Strand, L. D., Personal communication, Jet Propulsion Laboratory, September 1975.

6. Micci, M. M., Caveny, L. H., and Summerfield, M., "Solid Propellant Rocket Motor Responses Evaluated by Means of Forced Longitudinal Waves," AIAA Paper 77-974, July 1977.

7. Culick, F. E. C., "Stability of Longitudinal Oscillations with Pressure and Velocity Coupling in a Solid Propellant Rocket," Combustion Science & Technology, Vol. 2, 1970, pp. 179-201.

8. Levine, J. N. and Culick, F. E. C., "Numerical Analysis of Nonlinear Longitudinal Combustion Instability in Metallized Propellant Solid Rocket Motors. Vol. I: Analysis and Results," AFRPL-TR-72-88, July 1972.

9. Levine, J. N. and Culick, F. E. C., "Nonlinear Analysis of Solid Rocket Combustion Instability, Vol. I: Analysis and Results," AFRPL-TR-74-45, October 1974.

10. Kooker, D. E. and Zinn, B. T., "Numerical Solution of Axial Instabilities in Solid Propellant Rocket Motors," Proceedings of the 10th JANNAF Combustion Meeting, CPIA Publ. 243, Vol. I, December 1973, pp. 389-399.

11. Dehority, G. L. and Price, E. W., "Axial Mode, Intermediate Frequency Combustion Instability in Solid Propellant Rockets," NWC TP 5654, October 1974.

12. Battista, R. A., Caveny, L. H., and Summerfield, M., "Non-Steady Combustion of Solid Propellants," AMS Report No. 1049, Princeton University, Princeton, NJ, October 1972, pp. 7-8.

13. Lenoir, J. M. and Robillard, G., "A Mathematical Method to Predict the Effects of Erosive Burning in Solid Propellant Rockets," Sixth Symposium (International) on Combustion, Reinhold, NY, 1957, pp. 663-667.

14. Crump, J., "Behavior of Aluminum in Composite Propellants," from "Combustion of Solid Propellants and Low Frequency Combustion Instability," Naval Weapons Center, China Lake, CA, NOTS TP4244, June 1967.

15. Boggs, T. L., Mathes, H. B., Price, E. W., et al,"Combustion of Solid Propellants and Low Frequency Combustion Instability Progress Report," NWC TP 4749, Naval Weapons Center, China Lake, CA, June 1969.

16. Geisler, R. L., Kinkead, S. A., and Beckman, C. W., "The Relationship between Solid Propellant Formulation Variables and Motor Performance," AIAA Paper No. 75-1199, October, 1975, American Institute of Aeronautics and Astronautics, New York, NY.

17. Pokhil, P. F., Belyayev, A. G., Frolov, Yu. V., Logachev, V. A., and Korotkov, A. I., "Combustion of Powdered Metals in Active Media," FTD-MT-24-551-73, Translated from Russian by FTD.

18. Derr, R. L., Churchill, H. L., and Fleming, R. W., "Aluminum Behavior Near the Burning Surface of a Composite Propellant," Proceedings of 10th JANNAF Combustion Meeting, Vol. III. CPIA Publ. 243, Chemical Propulsion Information Agency, Silver Spring, MD, December 1973, pp. 327-339. Also, "Aluminum Behavior in Solid Propellant Combustion," Report AFRPL-TR-74-13, Air Force Rocket Propulsion Laboratory, Edwards, CA.

19. Gany, A., Caveny, L. H., and Summerfield, M., "Aluminized Solid Propellants Burning in a Rocket Motor Flow Field," AIAA Journal, Vol. 16, No. 7, July 1978, pp. 736-739.

20. Crump, J. E., Prentice, J. L., and Kraeutle, K. J., Combustion Science and Technology, Vol. 1, 1969, pp. 205-223.

21. Price, E. W. and Sigman, R. K., Georgia Institute of Technology, Atlanta, GA, AFOSR-TR-77-0050, November 1976.